

RESEARCH ARTICLE

# Reduction of Ca<sub>v</sub>1.3 channels in dorsal hippocampus impairs the development of dentate gyrus newborn neurons and hippocampal-dependent memory tasks

Su-Hyun Kim<sup>1,2</sup>, Ye-Ryoung Park<sup>1,2\*</sup>, Boyoung Lee<sup>3</sup>, Byungil Choi<sup>4</sup>, Hyun Kim<sup>4</sup>, Chong-Hyun Kim<sup>1,2\*</sup>

**1** Center for Neuroscience, Korea Institute of Science and Technology, Seoul, Korea, **2** Neuroscience Program, Division of Bio-Medical Science and Technology, KIST School, Korea University of Science and Technology, Seoul, Korea, **3** Center for Cognition and Sociality, Institute for Basic Science, Daejeon, Korea, **4** Department of Anatomy and Division of Brain Korea 21 Biomedical Science, College of Medicine, Korea University, Seoul, Korea

\* Current address: PRA Health Sciences, Gangnam-gu, Seoul, Korea

\* [ckimya@kist.re.kr](mailto:ckimya@kist.re.kr)



**OPEN ACCESS**

**Citation:** Kim S-H, Park Y-R, Lee B, Choi B, Kim H, Kim C-H (2017) Reduction of Ca<sub>v</sub>1.3 channels in dorsal hippocampus impairs the development of dentate gyrus newborn neurons and hippocampal-dependent memory tasks. *PLoS ONE* 12(7): e0181138. <https://doi.org/10.1371/journal.pone.0181138>

**Editor:** Giuseppe Gangarossa, University Paris Diderot, FRANCE

**Received:** March 18, 2017

**Accepted:** June 27, 2017

**Published:** July 17, 2017

**Copyright:** ©2017 Kim et al. This is an open access article distributed under the terms of the [Creative Commons Attribution License](https://creativecommons.org/licenses/by/4.0/), which permits unrestricted use, distribution, and reproduction in any medium, provided the original author and source are credited.

**Data Availability Statement:** All relevant data are within the paper and its Supporting Information files.

**Funding:** This work was supported by the Brain Research Program through the National Research Foundation of Korea (NRF) funded by the Ministry of Science, ICT & Future Planning (<http://www.nrf.re.kr/index>) to C.-H.K. (Project No. 2016M3C7A1905119 and 2015M3C7A1 028392) and by the KIST Institutional Program

## Abstract

Ca<sub>v</sub>1.3 has been suggested to mediate hippocampal neurogenesis of adult mice and contribute to hippocampal-dependent learning and memory processes. However, the mechanism of Ca<sub>v</sub>1.3 contribution in these processes is unclear. Here, roles of Ca<sub>v</sub>1.3 of mouse dorsal hippocampus during newborn cell development were examined. We find that knock-out (KO) of Ca<sub>v</sub>1.3 resulted in the reduction of survival of newborn neurons at 28 days old after mitosis. The retroviral eGFP expression showed that both dendritic complexity and the number and length of mossy fiber bouton (MFB) filopodia of newborn neurons at ≥ 14 days old were significantly reduced in KO mice. Both contextual fear conditioning (CFC) and object-location recognition tasks were impaired in recent (1 day) memory test while passive avoidance task was impaired only in remote (≥ 20 days) memory in KO mice. Results using adeno-associated virus (AAV)-mediated Ca<sub>v</sub>1.3 knock-down (KD) or retrovirus-mediated KD in dorsal hippocampal DG area showed that the recent memory of CFC was impaired in both KD mice but the remote memory was impaired only in AAV KD mice, suggesting that Ca<sub>v</sub>1.3 of mature neurons play important roles in both recent and remote CFC memory while Ca<sub>v</sub>1.3 in newborn neurons is selectively involved in the recent CFC memory process. Meanwhile, AAV KD of Ca<sub>v</sub>1.3 in ventral hippocampal area has no effect on the recent CFC memory. In conclusion, the results suggest that Ca<sub>v</sub>1.3 in newborn neurons of dorsal hippocampus is involved in the survival of newborn neurons while mediating developments of dendritic and axonal processes of newborn cells and plays a role in the memory process differentially depending on the stage of maturation and the type of learning task.

([https://www.kist.re.kr/kist\\_web/main/](https://www.kist.re.kr/kist_web/main/)) to C.-H.K. (Project No. 2E26820). The funders had no role in study design, data collection and analysis, decision to publish, or preparation of the manuscript.

**Competing interests:** The authors have declared that no competing interests exist.

## Introduction

L-type calcium channels (LTCCs) are formed by the Ca<sub>v</sub>1 family, which comprise isoforms of Ca<sub>v</sub>1.1–4 [1]. In neurons, both Ca<sub>v</sub>1.2 and Ca<sub>v</sub>1.3 are expressed [2] and are known to regulate neuronal excitability [3, 4], gene expression [5, 6], synaptic plasticity [3, 7–9], and learning and memory [10]. Pharmacological agents such as dihydropyridine derivatives have been used as blockers to find roles of LTCCs in hippocampal-dependent learning and memory [11–13]. However, it has been difficult to define functions of specific isoforms of LTCCs due to the non-specific sensitivity of blockers to isoforms of LTCCs and their toxicity [14]. Recently, genetic methods were used to investigate functions of each isoform in hippocampal-dependent learning and memory [15–20]. Ca<sub>v</sub>1.2 conditional KO (cKO) mice, where Ca<sub>v</sub>1.2 was deleted in the forebrain area including hippocampus and cortex, showed that consolidation of memory,  $\geq 3$  days old, of the Morris water-maze learning was defected [15, 17]. Null Ca<sub>v</sub>1.3 KO mice showed impairment in the recent memory of object location recognition (OLR) task [21] and CFC though there were no effects in extinctions at 2 to 3 days after training and in the recent memory of water-maze learning [16]. These genetic studies suggest differential roles of Ca<sub>v</sub>1.2 and Ca<sub>v</sub>1.3 even in hippocampal-dependent learning and memory tasks. Moreover, it is still unclear how hippocampal Ca<sub>v</sub>1.3 contributes to CFC learning and memory and whether the remote memory of CFC is affected or not in Ca<sub>v</sub>1.3 KO mice.

Adult hippocampal neurogenesis occurs in DG subgranular zone and has been suggested to be involved in the acquisition of new learning and memory processes [22, 23]. Ablation of adult hippocampal neurogenesis using x-ray irradiation or pharmacological methods has impaired hippocampal-dependent memories [24–28]. CFC memory is hippocampus-dependent [29] and survival of adult newborn neurons is shown important in single-trial CFC learning and memory [27, 28]. However, it is largely unknown what cellular and molecular mechanism could link the survival of adult newborn neurons with learning and memory processes. It has been shown that activity-dependent regulation of neurogenesis might be related with LTCCs [30–33]. Recently, reduction of survival of adult newborn neurons in adult hippocampus was observed in Ca<sub>v</sub>1.3 KO mice and forebrain-specific Ca<sub>v</sub>1.2 cKO mice [20, 34]. These studies suggest an idea that LTCCs can affect hippocampal-dependent learning and memory processes via their role in adult neurogenesis. Therefore, it will be interesting to know what endogenous functions of Ca<sub>v</sub>1.3 have in the development of adult newborn neurons, which can be critical for learning and memory.

In this study we aimed to determine what developmental stages of adult hippocampal neurogenesis are directly affected by Ca<sub>v</sub>1.3, how Ca<sub>v</sub>1.3 regulates the development of adult newborn neurons, and in what region, such as dorsal vs ventral, of hippocampus Ca<sub>v</sub>1.3 is important for CFC learning. To achieve these aims, hippocampal neurogenesis was quantified along a month period of time and the morphology of dendrites and axon terminals of DG newborn neurons of Ca<sub>v</sub>1.3 KO mice was investigated. To confirm the effect of hippocampal-dependent memory tasks in KO mice, effects of AAV- or retrovirus-mediated Ca<sub>v</sub>1.3 KD of dorsal hippocampal area on learning and memory tasks were examined. The results showed that Ca<sub>v</sub>1.3 in dorsal hippocampal newborn neurons affects the survival and development of newborn neurons and is involved in the recent CFC memory, and Ca<sub>v</sub>1.3 in mature neurons seems to contribute to both recent and remote memory of CFC learning.

## Materials and methods

### Animals

The animal procedures were in accordance with the guidance of the principles in the care and use of experimental animals which were set by the Animal Care and Use Committee of Korea

Institute of Science & Technology (ACUCK) and all animal experiments were approved by ACUCK done in this study where male 8 to 12 week old mice were used. In the Ca<sub>v</sub>1.3 KO mice, the gene for the pore-forming subunit of the Ca<sub>v</sub>1.3 calcium channel has been deleted by insertion of a neomycin cassette into exon 2, which results in a complete null mutation [35]. Mice were maintained in two genetic backgrounds, either 129/sv or C57BL/6J. KO and WT littermate mice were generated by mating heterozygotes from two genetic backgrounds (129/sv and C57BL/6J). All animals were kept at 23 ~ 25°C under light/dark (12:12 hour) cycle and given *ad libitum* access to food and water.

## Production of AAV and retrovirus

Candidate shRNAs targeting Ca<sub>v</sub>1.3 were, 24 base pair sequence long, designed by RNAi design program (Integrated DNA Technologies). A loop sequence (CTTCCTGTCA) was inserted between antisense (TTATCTCTCATGGCAACTTCCCA) and sense (TGGGAAAGTTGCCATGAGAGATAAAA) sequences. DNA oligomers were synthesized and cloned into a modified pAAV-MCS vector, pAAV-shRNA (provided by Dr. Ralph J. DiLeone, Yale University School of Medicine). The insertion was confirmed by sequencing and the best candidate was selected by measuring KD efficiency with quantitative real-time polymerase chain reaction (qRT-PCR) after transfecting candidate plasmids into primary neuronal culture. KD control GFP-AAV carries a scrambled shRNA sequence. To produce high titer AAV ( $1 \times 10^9 \sim 10^{11}$  pfu/ml), the target plasmid, pRC and pHelper plasmids (gift from Dr. R. J. Dileone), were transiently transfected to HEK293TN cells. Cell lysates harvested at 72 hours after transfection were treated with benzonase (50 unit/ml; Sigma, USA) and virus particles were purified and concentrated with heparin column (GE healthcare, Sweden) and 100k filtering tube (Millipore, USA). Virus titers were determined by counting GFP (+) HEK293T cells at 48 hours after infection. Retroviral vector (CAG-GFP, gift from Dr. Fred H. Gage, Salk Institute, USA) was used for making retrovirus to label adult newborn neurons of DG area of mouse [36]. To KD Ca<sub>v</sub>1.3, Ca<sub>v</sub>1.3 targeting shRNA candidates, 19 base pair sequence long, were designed by RNAi design program (IDTdna, USA). A loop sequence (TTCAAGAGA) was inserted into between sense (GGCCCGCGTTGCTGTACAA) and antisense (TTGTACAGCAACGCGGGCC) sequences.

DNA oligomers were synthesized and cloned into the retrovirus plasmid (RNAi-Ready pSIREN-RetroQ vector, Clontech, Japan). The insertion was confirmed by sequencing and KD efficiency was measured by qRT-PCR at 48 hours after transfection into HT22 cell line. KD control GFP-retrovirus carries a scrambled shRNA sequence. To change or enhance the fluorescence of retrovirus, Ca<sub>v</sub>1.3 targeting shRNAs were subcloned into pSUBGW plasmids (gift from Dr. H. Song, Johns Hopkins University, USA). To produce high titer retrovirus, retroviral vector and VSVG (gift from Dr. F. H. Gage) were transiently transfected to HEK293-based packaging cell line (Platinum-GP Retroviral Packaging Cell Line, Cell Biolabs, USA) and media were changed and collected at every 24 hour interval for 3 days after transfection (S6C and S6D Fig).

## Quantitative real-time polymerase chain reaction

Total cellular RNA was isolated from cells using the total RNA extraction kit or manually using trizol (Geneall, Korea). qRT-PCR was done using a real time PCR system (Applied Biosystems: 1 cycle at 50°C for 2 min & 95°C for 10 min; 40 cycles at 95°C for 15 s & 60°C for 1 min). Glyceraldehyde 3-phosphate dehydrogenase was used as a control for cDNA loading and PCR. PCR primers were synthesized by M-biotech Inc. (Korea). Ca<sub>v</sub>1.3 PCR primers were targeted to exon 21–22 (# Mm.PT.47.16004990).

## Stereotaxic viral injections

AAV (2  $\mu$ l) or retrovirus (1.5  $\mu$ l) containing solution was injected into the molecular layer of the DG (Dorsal hippocampus, anterior-posterior (AP): -2.0 mm, medial lateral (ML):  $\pm$ 1.5 mm, dorsal ventral (DV): -1.85 mm; Ventral hippocampus, AP: -2.8 mm, ML:  $\pm$ 3 mm, DV: -4 mm) using microsyringe pump (Micro 4, WPI, USA) and a calibrated 50  $\mu$ l Hamilton syringe (Hamilton co., USA) fitted with a 33-gauge needle (WPI, USA) (0.1  $\mu$ l/min). Mice were anesthetized with a mixture of avertin (200 mg/kg; Sigma, USA) and placed in a stereotaxic frame (Stoelting Co, USA). The final titers of retrovirus and AAV were  $\sim$ 10<sup>8</sup> pfu/ml and 10<sup>9</sup> ~ 10<sup>11</sup> pfu/ml, respectively.

## Immunohistochemistry (IHC)

Bromodeoxyuridine (BrdU, Sigma, USA) was used to quantify the proliferation and survival of adult newborn neurons of DG in hippocampus. To quantify the proliferation rate of newborn neurons, mice were injected with BrdU (300 mg/kg in saline) once intraperitoneally and sacrificed at 24 hours after the BrdU injection. To quantify the survival rate of newborn neurons, mice were injected with BrdU (300 mg/kg in saline) once a day for 4 days intraperitoneally and sacrificed at 14 or 28 days after the last BrdU injection. For perfusion of brain, mice were anesthetized with avertin (200 mg/kg, Sigma) and transcardially perfused with cold 0.1M phosphate buffer saline (PBS) and then 10% neutral buffer formalin (NBF, Sigma). Brains were post-fixed overnight in 10% NBF at 4°C, then cryoprotected in 30% sucrose in PBS at 4°C for 2 days. Coronal section of 40  $\mu$ m thick was cut using cryostat (HM525, Thermo scientific, USA). For immunostaining of BrdU, brain sections were pretreated 2 N HCl for 1 hour at 37°C and rinsed in 0.1 M borate buffer (pH 8.5) for 10 min. To block non-specific bindings, sections were incubated in 2% normal goat serum with 0.3% triton X-100 in PBS (Blocking solution) for 1 hour at room temperature (RT) and then incubated in rat anti-BrdU antibody (1:400, Serotec, USA) and mouse anti-NeuN antibody (1:400, Millipore, USA) in blocking solution for 16 hours at 4°C. After incubation, sections were washed in PBS and incubated in goat anti-rat 488 (1:400, life technology, USA) and goat anti-mouse 568 (1:400, Life technology, USA) antibodies in blocking solution for 2 hours at RT. For immunostaining of Ca<sub>v</sub>1.3 in mouse brain, animals were perfused with cold PBS and post-fixed with 10% NBF for 1 hour at RT. Sections were washed 3 times, each 10 min in 0.1 M PBS and then incubated in 4% normal goat serum (NGS, Vector laboratories, USA) in PBS containing 0.25% triton-X100 for 2 hours at RT. Then sections were incubated in rabbit anti-Ca<sub>v</sub>1.3 (1:200, Alomone Lab, Israel) in blocking solution for 72 hours at 4°C, washed in PBS and incubated in secondary antibodies in PBS containing 0.25% triton-X100 for 2 hours at RT.

## Image acquisition and analysis

Images were acquired using a confocal microscope (Fluoview 1000, Olympus, Japan). Retrovirus expressing eGFP was used to label adult newborn neurons [36]. Images of GFP (+) cells were acquired at 14 or 28 days after viral injection into dorsal hippocampal region. Images (40x objective lens), taken in 1  $\mu$ m step, were used for detecting BrdU (+) cells and for analysis of morphology of dendrites of newborn neurons. Images (40x/6x-zoom) in 1  $\mu$ m step were used to analyze the morphology of axon terminals. Images (60x/6x-zoom) were used to analyze the spine morphology and density. Fiji software (Image J, NIH, USA) was used to measure, reconstruct and analyze the length, complexity, branching points of dendrites and axon terminal morphology. NeuronStudio software (<http://www.mssm.edu/cnic>) was used to analyze the dendritic spine morphology and density of GFP (+) neurons [37]. The types of spine were



classified as stubby, thin or mushroom by using the default values of the software (Neck Ratio, 1.1; Thin Ratio, 2.5; Mushroom size, 0.35  $\mu$ m).

## Animal behavior experiments

**Contextual fear conditioning (CFC).** The procedure for testing CFC memory was in accordance with the method of McKinney et al. (2006) [16]. Fear conditioning was carried out in the chamber (18 x 17.5 x 38 cm) (Med Associates, USA) containing a stainless-steel bar-grid floor (5 mm  $\phi$  rods, spaced 1 cm apart). Electric shock was delivered through the bar-grid floor of the box connected to a programmable shocker. A light bulb and a fan were located inside the chamber. Every mouse was handled for 3 min per day for 5 days before the training session of CFC. On the 1<sup>st</sup> training day (Day 0), mouse was given with a single shock (0.5 mA, 2 s) at 180 s after exposure to the chamber and then was returned to the home cage 30 s after the shock. Intensity of light bulb illumination inside chamber was 30 ~ 50 lux. At 24 hours after the 1<sup>st</sup> training, the 2<sup>nd</sup> training procedure was given while video recording the freezing behavior (Day 1). On the 3<sup>rd</sup> day, mouse was placed in the same chamber for CFC memory test (Day 2). To assess the remote memory of CFC, freezing behavior was monitored for 3 min at 23 days after the 1<sup>st</sup> training day.

**Passive avoidance (PA).** The PA procedure of PA was described in Pan et al. (2012) [38]. In brief, on the training day (Day 0) mouse was placed in the lighted compartment, facing away from the dark compartment and the guillotine door was lifted open after 30 s free exploration. When mouse entered the dark compartment along with all four paws, the guillotine door was closed and the latency to enter was recorded (from the time when the door was lifted). A foot-shock was delivered (0.7 mA, 2 s) at 3 s after closing the door and 30 s later, the mouse was moved to the home cage. To measure the recent memory of PA learning, at 24 hours after the training, the mouse was returned to the lighted compartment, facing away from the dark compartment. After 30 s later, the guillotine door was open. Latency to enter the dark compartment was measured (Day 1). To measure the remote memory of PA, the latency was recorded at 21 and 42 days after the training day. Measurements at day 42 used mice only that did show the shock memory at day 21.

**Object recognition (OR) and OLR tasks.** Procedures of OR and OLR were based on Goodman et al. (2010) [21]. OR task was performed in an open field box (40 x 40 x 40 cm). Two types of objects were different in shape, color and texture. One of them was a yellow regular tetrahedron, made of acryl. The other one was a black & red color sphere, made of urethane. Both are 7 ~ 7.5 cm high. The objects were fixed to the ground of the box, not to be moved by mice. Sniffing objects was considered as the explorative action of mouse. OR test was composed of 3 steps such as habituation, training and test, and given once per day. During the habituation step, mouse was placed in an open field box for 30 min without objects. Then, during training period, two identical objects were presented to the mouse for 20 min. At 24 hours after the training, one of the familiar objects was replaced with a novel object and presented to the mouse for 10 min for the test. Procedures for OLR task were similar to OR task except that one of the objects was moved to a different location for the test.

## Statistics

Statistical values are presented as means  $\pm$  S.E. and two-tailed unpaired t-test with  $\alpha = 0.05$  was used to compare data between two experimental groups unless otherwise mentioned. One-way or two-way ANOVA was applied to most analysis if applicable and post hoc (Bonferroni or Dunnett) analysis was followed (SPSS v.24, IBM, USA). G = genotype, T = time or trials,

D = distance, S = Sound dB. The results of ANOVA and post hoc analysis were provided in Supporting Information.

## Results

### Expression of Ca<sub>v</sub>1.3 in newborn neurons as well as mature neurons

Ca<sub>v</sub>1.3 is expressed in various regions of the brain such as cortex, hippocampus, lateral ventricle, cerebellum, olfactory bulb, and thalamus [39, 40]. *In situ* results confirmed the broad existence of Ca<sub>v</sub>1.3 mRNA in mouse brains of embryo to adult (S1A Fig). Immunohistochemistry of Ca<sub>v</sub>1.3 showed the strong expression in cell body regions compared to dendritic and axonal regions of neurons in *Cornu Ammonis 1* (CA1), CA3 and DG of dorsal hippocampus and cortex of adult mice (Fig 1A and S1B Fig), which is consistent with Veng and Browning (2002) [41]. Previous study with a mouse line expressing Ca<sub>v</sub>1.3 tagged with eGFP showed co-labeling of Ca<sub>v</sub>1.3 with NeuN (+) cells and some of nestin (+) or GFAP (+) cells but little co-labeling with DCX (+) cells, suggesting a differential expression of Ca<sub>v</sub>1.3 during development of neural stem cells (NSCs) in DG [20]. To check how Ca<sub>v</sub>1.3 is expressed in newborn neurons of DG, GFP-retrovirus was injected to infect newborn cells. The results showed that Ca<sub>v</sub>1.3 expression of newborn neurons 3 to 7 days old was about half level of mature neurons and started to increase after Day 7 (Fig 1B and 1C). Ca<sub>v</sub>1.3 immuno-fluorescent intensities at 14 and 28 day old cells were increased by ~52% and ~74% over that of 7 day old cells, respectively (Fig 1D), suggesting that new Ca<sub>v</sub>1.3 expression was strongly triggered between 7 and 14 day old period. However, the fluorescent intensity of Ca<sub>v</sub>1.3 from cell bodies of newborn neurons of ≤ 28 days old was still significantly weaker than that of mature granule neurons (GFP (-) cells) (Fig 1D). Co-immunostaining of DCX and Ca<sub>v</sub>1.3 in WT mice shows that DCX (+) mature cells with tertiary dendrites have higher Ca<sub>v</sub>1.3 expression in the cell body than DCX (+) immature cells (S2A–S2C Fig). Within hippocampal regions, cell body Ca<sub>v</sub>1.3 intensity was stronger in CA3 region than those in CA1 and DG areas by ~10% and ~19%, respectively (Fig 1E). The results show that Ca<sub>v</sub>1.3 is expressed in both newborn cells and mature neurons and the expression is low initially and then after 7 days old keeps increasing until adult stage.

### Reduction of the survival rate of hippocampal newborn neurons in Ca<sub>v</sub>1.3 KO mice

A recent study reported that survival of adult newborn neurons 28 days old was reduced in Ca<sub>v</sub>1.3 KO mice [20]. However, it is unclear when the survival rate of newborn neurons in KO mice starts to change differentially. We first confirmed KO of Ca<sub>v</sub>1.3 (S1C–S1D Fig) and deafness of KO mouse (S1E Fig). To look into the time course of development of newborn cells, the number of DG newborn cells of dorsal hippocampus of KO mice was analyzed at following days after BrdU injection; 1 day for proliferation, 14 day for the early survival and 28 day for the late survival (Fig 2A). The newborn cell numbers at day 1 and day 14 were not different between WT and KO mice. At day 28, even in WT mice, the number of BrdU (+) cells was reduced by ~42% compared to that of day 14 (Fig 2B). In KO mice, the number of BrdU (+) cells at day 28 was further reduced in KO mice by ~27% compared to that of WT (Fig 2C), suggesting a contribution of Ca<sub>v</sub>1.3 on the survival of newborn neurons. The density of BrdU (+) cells per DG area at day 28 was also reduced in KO mice by ~27% (Fig 2D). Analysis of DCX (+) cells showed that the total number of DCX (+) cells was not changed in KO mice but percentage of mature cells selectively decreased in KO mice (S2D–S2F Fig). Works on the correlation between the survival of newborn cells and the area/volume of DG have been controversial [20, 34, 42]. Studies by Marshallinger et al. (2015) and Noto et al. (2016) showed that the

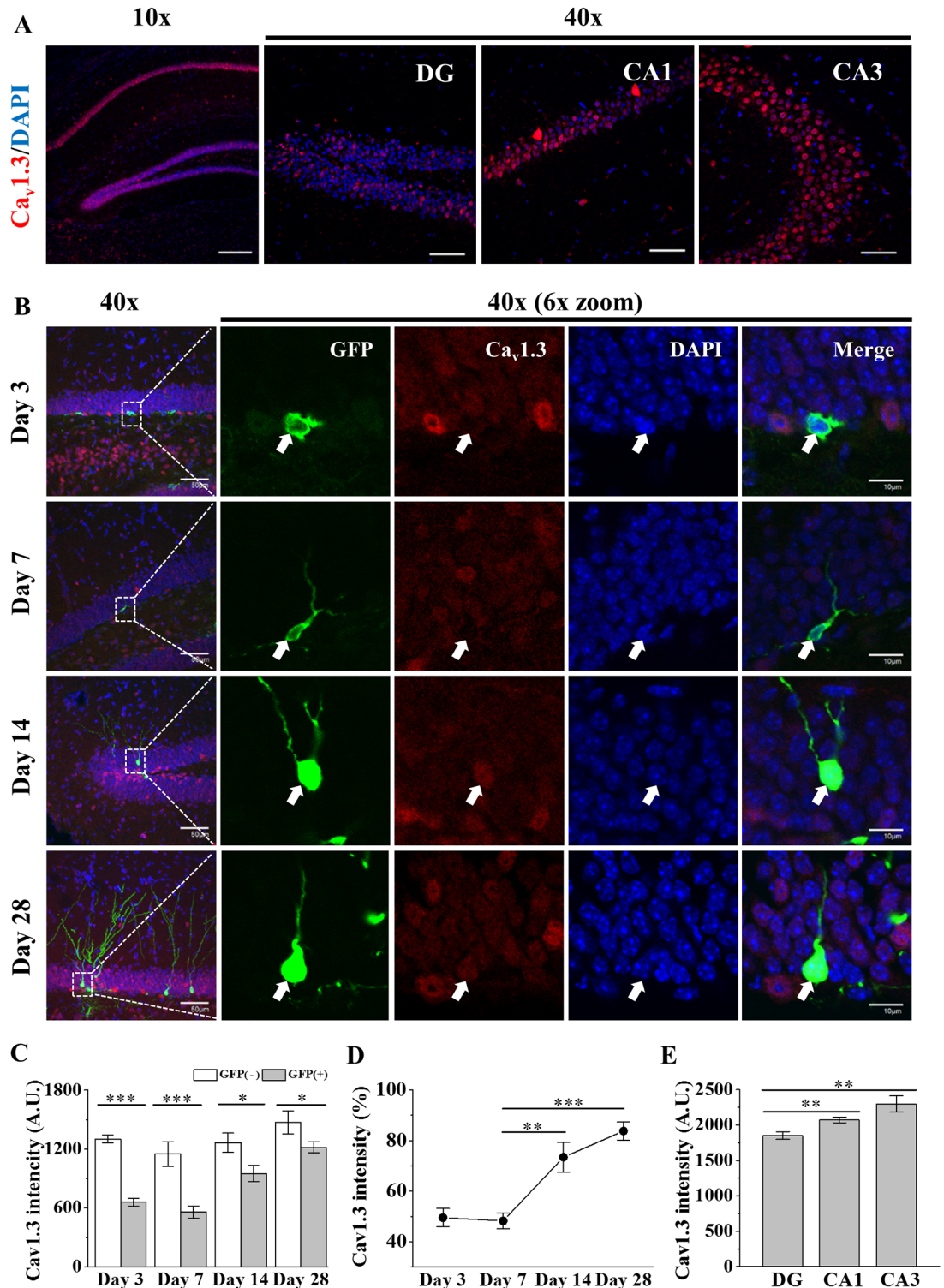


**Fig 1. Expression of Ca<sub>v</sub>1.3 in adult hippocampal area.** (A) Ca<sub>v</sub>1.3 expression in dorsal hippocampal area. Ca<sub>v</sub>1.3 is shown in red and DAPI, a nuclear marker, is shown in blue. Scale bars, 200 μm (10x) and 50 μm (40x). (B) Images of developmental profiling of Ca<sub>v</sub>1.3 expression in adult hippocampal newborn neurons. Confocal images of adult hippocampal newborn neurons, infected with GFP-retrovirus and stained with Ca<sub>v</sub>1.3 antibody (red), were taken at 3, 7, 14 and 28 days after infection. White arrows indicate newborn cells infected with retrovirus. Scale bars, 50 μm (40x) and 10 μm (40x/6x-zoom). (C) Ca<sub>v</sub>1.3 antibody fluorescent intensity of newborn neurons (GFP (+), filled bar) and control (GFP (-), open bar) at 3, 7, 14 and 28 days after infection. (D) Ca<sub>v</sub>1.3 antibody fluorescent intensity of newborn neurons (GFP (+)) at 3, 7, 14 and 28 days after infection. (E) Ca<sub>v</sub>1.3 antibody fluorescent intensity of newborn neurons (GFP (+)) in DG, CA1 and CA3 regions. Statistical significance is indicated by asterisks: \*\*\* p < 0.001, \*\* p < 0.01, \* p < 0.05.

mature neurons (GFP (-), open bar) of dorsal hippocampus shown at (B). A.U. indicates arbitrary unit. (Day 3, GFP(+),  $658.10 \pm 41.58$ ,  $n = 9$ , GFP(-),  $1302.51 \pm 40.98$ ,  $n = 50$ ; Day 7, GFP(+),  $558.19 \pm 61.26$ ,  $n = 9$ , GFP(-),  $1149.03 \pm 126.35$ ,  $n = 50$ ; Day 14, GFP(+),  $950.79 \pm 83.09$ ,  $n = 7$ , GFP(-),  $1264.75 \pm 97.98$ ,  $n = 50$ ; Day 28, GFP(+),  $1217.75 \pm 55.34$ ,  $n = 13$ , GFP(-),  $1470.64 \pm 115.84$ ,  $n = 50$ ;  $p(\text{Day } 3) < 0.000$ ,  $p(\text{Day } 7) = 0.000$ ,  $p(\text{Day } 14) = 0.035$ ,  $p(\text{Day } 28) = 0.041$ ). Two-way ANOVA,  $F_G = 66.17$ ,  $p = 0.000$ ;  $F_T = 15.22$ ,  $p = 0.000$ ;  $F_{G+T} = 3.20$ ,  $p = 0.031$ . (D) Normalized Ca<sub>v</sub>1.3 antibody fluorescent intensity of newborn neurons to that of mature neurons. (Day 3,  $49.52 \pm 3.61\%$ ,  $n = 9$ ; Day 7,  $48.26 \pm 3.08\%$ ,  $n = 9$ ; Day 14,  $73.42 \pm 5.94\%$ ,  $n = 7$ ; Day 28,  $83.76 \pm 3.58\%$ ,  $n = 13$ ;  $p(\text{Day } 3-7) = 0.795$ ,  $p(\text{Day } 7-14) = 0.001$ ,  $p(\text{Day } 14-28) = 0.138$ ). One-way ANOVA,  $F = 20.913$ ,  $p = 0.000$ . (E) Comparison of Ca<sub>v</sub>1.3 expression among DG, CA1 and CA3 regions of dorsal hippocampus shown at (A) (each,  $n = 10$ ). (DG,  $1851.50 \pm 54.44$ ,  $n = 10$ ; CA1,  $2072.08 \pm 38.63$ ,  $n = 10$ ; CA3,  $2298.10 \pm 115.40$ ,  $n = 10$ ;  $p(\text{DG-CA1}) = 0.004$ ,  $p(\text{CA1-CA3}) = 0.080$ ,  $p(\text{DG-CA3}) = 0.003$ ). One-way ANOVA,  $F = 8.42$ ,  $p = 0.001$ . \*, \*\*, \*\*\* indicate  $p < 0.05$ ,  $p < 0.01$ ,  $p < 0.001$ , respectively.

<https://doi.org/10.1371/journal.pone.0181138.g001>

change of the survival rate of newborn cells was positively related with that of the volume of DG in Ca<sub>v</sub>1.3 KO and 5-HT<sub>1A</sub>R overexpressing transgenic mice, respectively, but Lee et al. (2016) showed that the survival of newborn cell was increased in the absence of the change in DG area in Ca<sub>v</sub>1.2 forebrain KO mice. We measured DG area and the area and density of granule cells in KO mouse using NeuN antibody (see [Methods](#)). The results showed that areas of DG and granule cell layer and the density of mature granule cells were not significantly changed at day 28 in KO mice ([Fig 2F-2H](#)).

### Impairments of dendritic and MFB growth and MFB filopodia development of hippocampal newborn neurons in Ca<sub>v</sub>1.3 KO mice

Adult hippocampal newborn neurons grow substantially during 14 to 28 day old period after mitosis [36]. The correlation of this period with the time for survival or synaptic integration of newborn neurons in DG has been suggested [32, 43, 44]. In this study, we have adopted retrovirus labeling to analyze morphological development of dendrites and MFB, MFB filopodia and dendritic spines of newborn neurons of dorsal hippocampus of Ca<sub>v</sub>1.3 KO mice [36]. Exemplary images of GFP (+) dendritic processes of newborn neurons were shown in [Fig 3A](#). The numbers of total branching points of dendrites of newborn neurons at day 14 and day 28 in KO mice were significantly reduced by ~14% and ~26%, respectively, compared with those of WT mice ([Fig 3B](#)). The total dendritic length of newborn neurons at day 28 was also significantly reduced by ~16% in KO mice ([Fig 3C](#)). To examine the dendritic complexity of newborn neurons, Sholl analysis was applied with Fiji program [45] ([Fig 3D and 3E](#)). The dendritic complexity within range of 100 μm from soma of newborn neurons at day 28 was significantly reduced by 12 ~ 22% in KO mice ([Fig 3E](#)). These results together suggest that both the appearance of initial dendrites from the soma and the activity of branching and growth of dendrites of newborn neurons in KO mouse seem quite normal until 14 days old, when most dendrite length is shorter than 100 μm, but when it is over 14 days old, the appearance of new dendrites from the soma or the activity of their branching and growth gets slower or inhibited although preexisting dendrites seem to keep growing normally over 100 μm long in KO mice. It is possible that higher expression of Ca<sub>v</sub>1.3 in newborn neurons ≥ 14 days old could be related with the later dendritic development.

During functional synapse formation, the morphology of spines might change from thin filopodia to stubby to mature mushroom types [36, 46]. LTCCs have been reported to contribute to calcium signaling in dendritic spines [47, 48]. However, it is largely unknown about roles of LTCCs in dendritic spine formation. Recently, it has been shown that splice variants of Ca<sub>v</sub>1.3 regulated the morphology of dendritic spines of cultured hippocampal neurons [49]. Therefore, to check an effect of Ca<sub>v</sub>1.3 in the spine development of adult newborn neurons *in vivo*, morphological types of dendritic spines were analyzed ([Fig 3F](#)). The results showed that the



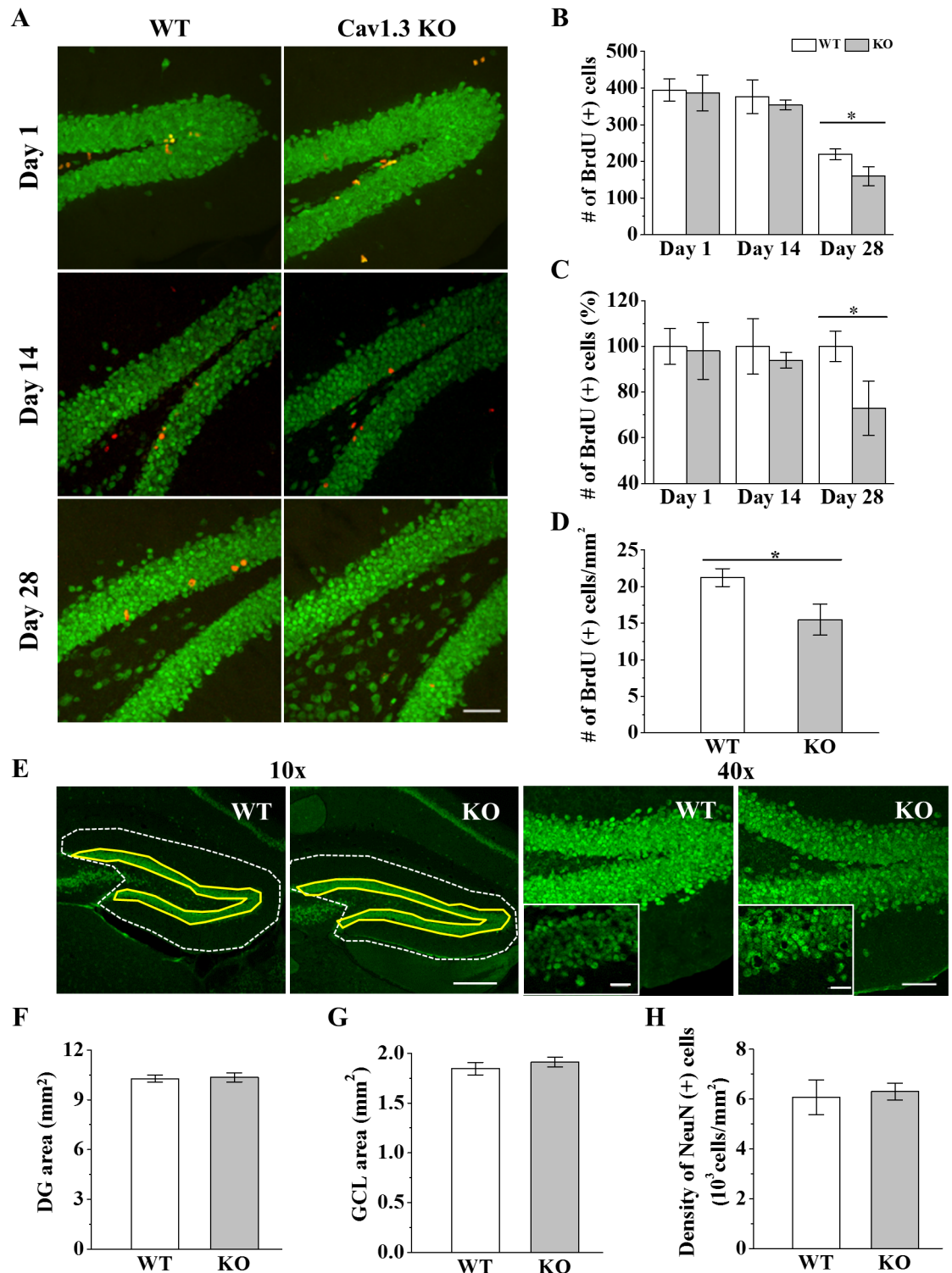


**Fig 2. Proliferation and survival of DG newborn cells of dorsal hippocampus in Ca<sub>v</sub>1.3 KO mouse.** (A) Confocal images of BrdU (+) cells (red) and NeuN (+) cells (green) in Ca<sub>v</sub>1.3 KO and WT mouse. Images are acquired at 1, 14 and 28 days after BrdU injection. *Scale bar*, 50  $\mu$ m. (B) Number of BrdU (+) cells. (Day 1, WT, 394.667  $\pm$  30.78 cells, n = 8; KO, 387  $\pm$  49.05, n = 6,  $p$  = 0.660; Day 14, WT, 376.6  $\pm$  45.85 cells, n = 6; KO, 35.8  $\pm$  13.22 cells, n = 6,  $p$  = 0.472; Day 28, WT, 219  $\pm$  13.61 cells, n = 7; KO, 159.83  $\pm$  23.70 cells, n = 6,  $p$  = 0.046). \* indicates  $p$  < 0.05. Two-way ANOVA,  $F_G$  = 3.80,  $p$  = 0.061;  $F_T$  = 59.12,  $p$  = 0.000;  $F_{G+T}$  = 0.84,  $p$  = 0.444. (C) Number of BrdU (+) cells of KO mice normalized to that of WT mice at given day. (Day 1, WT, 100  $\pm$  7.80%, n = 8, KO, 98.06  $\pm$  12.43%, n = 10; Day 14, WT, 100  $\pm$  12.17%, n = 6,



KO,  $93.95 \pm 3.50\%$ ,  $n = 6$ ; Day 28, WT,  $100 \pm 6.73\%$ ,  $n = 7$ , KO,  $72.98 \pm 11.85\%$ ,  $n = 6$ ,  $p = 0.046$ ). Two-way ANOVA,  $F_G = 4.61$ ,  $p = 0.040$ ;  $F_T = 1.82$ ,  $p = 0.179$ ;  $F_{G+T} = 1.90$ ,  $p = 0.168$ . (D) Number of BrdU (+) cells per DG area at Day 28. (WT,  $21.24 \pm 1.22$  cells/mm<sup>2</sup>,  $n = 7$ ; KO,  $15.47 \pm 2.12$ ,  $n = 6$ ,  $p = 0.032$ ). (E) *Left*, example images for area measurements of DG (white dot line) and GCL (yellow line). *Right*, NeuN (+) cells (green) of DG in  $Ca_v1.3$  KO and WT mice. *Scale bars*, 100  $\mu$ m (10x), 50  $\mu$ m (40x), 10  $\mu$ m (*insets*, 40x/5x-zoom). (F) DG area (WT,  $9.92 \pm 0.19$  mm<sup>2</sup>,  $n = 6$ , KO,  $9.58 \pm 0.18$  mm<sup>2</sup>,  $n = 6$ ,  $p = 0.833$ ), (G) GCL area (WT,  $1.85 \pm 0.063$  mm<sup>2</sup>,  $n = 6$ , KO,  $1.91 \pm 0.05$  mm<sup>2</sup>,  $n = 7$ ,  $p = 0.445$ ) and (H) Density of NeuN (+) cells in GCL (WT,  $6071 \pm 691.88$  cells/mm<sup>2</sup>,  $n = 11$ , KO,  $6304.71 \pm 339.34$  cells/mm<sup>2</sup>,  $n = 12$ ,  $p = 0.897$ ).

<https://doi.org/10.1371/journal.pone.0181138.g002>

density of thin, stubby, mushroom types of spines of adult newborn neurons at day 28 was not changed significantly (Fig 3G). The result suggests that the effect of  $Ca_v1.3$  deletion of newborn neurons on spine development marginally occurs over 14 days old, if any, when functional dendritic spine formation occurs usually, further coinciding with the survival period of newborn neurons [36].

Newborn neurons also generate axonal fibers and make synaptic contacts with target neurons including hilar interneurons, CA3 pyramidal cells and interneurons when they are 17 to 28 days old [50–53]. Synapse formation could contribute to the dendritic maturation of newborn neurons [44, 54]. While the filopodia of the mossy terminals interact mainly with the GABAergic interneurons, MFBs form synapses on excitatory pyramidal cells and hilar mossy cells [55]. To find a role of  $Ca_v1.3$  on axonal development and possibly synapse formation, filopodia and the size of axonal boutons of newborn neurons in CA3 regions at day 28 were characterized in KO mice (Fig 3H). The size of MFB was decreased by ~13% in KO mice (Fig 3I). The total number and total length of filopodia per bouton were significantly smaller in KO mice by ~25% and ~27%, respectively (Fig 3J and 3K).

The result of morphological analysis of newborn neurons suggests that  $Ca_v1.3$  is mainly necessary for the proper development of both dendrite and axonal fibers and might contribute to the formation of functional synapses and thereby, possibly for the survival of newborn neurons.

### Shock sensitivity, locomotion, anxiety level, visual function and working memory seem normal in $Ca_v1.3$ KO mice

$Ca_v1.3$  is expressed in various cell types of mouse organs such as retina, inner hair cells, heart and pancreas [39, 56–59]. Therefore, to check whether null KO of  $Ca_v1.3$  in mouse might cause any serious neurobiological effects, some critical neurological screening tests were done before executing behavioral experiments. First of all, we confirmed the deafness of KO mice (S1E Fig) shown in [35, 60], which made us to use CFC rather tone-fear conditioning. Second, to examine the sensitivity to electrical shocks, responses to shocks were categorized such as flinch, vocalization and jump after the shock (S3A Fig) [61]. The results showed for the first time that thresholds of responses to shocks in all three categories were not significantly different between KO and WT mice, indicating the normal sensitivity to shocks of KO mice. Third, the effect on body weight in  $Ca_v1.3$  KO mice has been debated [16, 60]. We found body weights of KO mice were slightly less by ~7% in 8-week old KO mice (S3B Fig), and the biological significance of the difference was not pursued. Fourth, to measure both the locomotor activity and the anxiety level, open field test was made. The results showed no significant difference in the total moving distance and in the ratio of the moving distance within the center area over the total moving distance (S3C and S3D Fig), indicating normal locomotor activity and anxiety level in KO mice. Fifth, to test the working memory, Y-maze test was applied. The total number of entries and the percentage of spontaneous alternation were not significantly different between KO and WT mice, suggesting normal working memory capability of KO

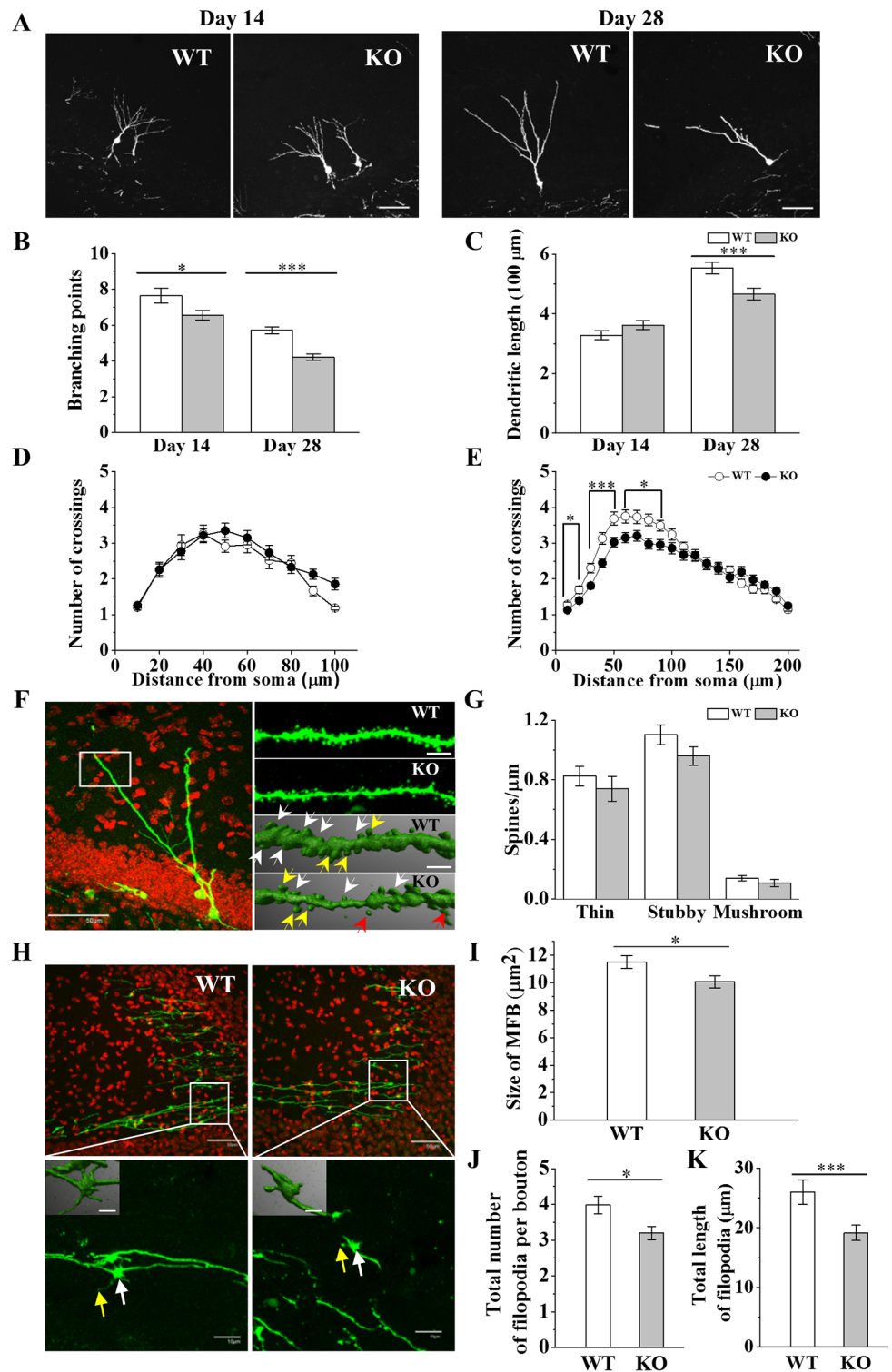


**Fig 3. Effects of Ca<sub>v</sub>1.3 KO on developments of dendrites, spines and MFB filopodia of DG newborn neurons.** (A) Confocal images of GFP (+) neurons at 14 and 28 days after GFP-retroviral infection. Scale bar, 50 μm. (B-E) Quantification of dendritic development. \*, \*\*, \*\*\* indicate  $p < 0.05$ ,  $p < 0.01$ ,  $p < 0.001$ , respectively. (B) Total number of dendritic branching points at 14 and 28 days after viral infection. (Day 14, WT,  $7.64 \pm 0.41$ ,  $n = 62$ , KO,  $6.55 \pm 0.25$ ,  $n = 102$ ,  $p = 0.017$ ; Day 28, WT,  $5.71 \pm 0.20$ ,  $n = 107$ , KO,  $4.20 \pm 0.18$ ,  $n = 120$ ,  $p < 0.00001$ ,  $n = 3$  animals per group). Two-way ANOVA,  $F_G = 26.96$ ,  $p = 0.000$ ;

$F_T = 73.08, p = 0.000; F_{G+T} = 0.68, p = 0.001$ . (C) Total dendritic length measurement at 14 and 28 days after viral injection. (Day 14, WT,  $328.35 \pm 14.57 \mu\text{m}$ ,  $n = 69$ , KO,  $362.34 \pm 45.06 \mu\text{m}$ ,  $n = 100, p = 0.12$ ; Day 28, WT,  $552.90 \pm 19.15 \mu\text{m}$ ,  $n = 107$ , KO,  $466.34 \pm 19.97 \mu\text{m}$ ,  $n = 119, n = 4$  animals per group,  $p = 0.002$ ). Two-way ANOVA,  $F_G = 1.96, p = 0.162; F_T = 76.56, p = 0.000; F_{G+T} = 10.31, p = 0.001$ . (D-E) Number of dendritic crossings in Sholl analysis at 14 (D) and 28 days (E) after viral infection. (Day 28:  $10 \mu\text{m}$ , WT,  $1.29 \pm 0.07$ , KO,  $1.13 \pm 0.04, p = 0.022$ ;  $20 \mu\text{m}$ , WT,  $1.70 \pm 0.10$ , KO,  $1.39 \pm 0.07, p = 0.011$ ;  $30 \mu\text{m}$ , WT,  $2.30 \pm 0.13$ , KO,  $1.81 \pm 0.09, p = 0.001$ ;  $40 \mu\text{m}$ , WT,  $3.13 \pm 0.16$ , KO,  $2.44 \pm 0.11, p = 0.001$ ;  $50 \mu\text{m}$ , WT,  $3.69 \pm 0.18$ , KO,  $3.03 \pm 0.13, p = 0.004$ ;  $60 \mu\text{m}$ , WT,  $3.75 \pm 0.18$ , KO,  $3.15 \pm 0.14, p = 0.010$ ;  $70 \mu\text{m}$ , WT,  $3.73 \pm 0.19$ , KO,  $3.21 \pm 0.15, p = 0.025$ ;  $80 \mu\text{m}$ , WT,  $3.65 \pm 0.16$ , KO,  $2.98 \pm 0.14, p = 0.005$ ;  $90 \mu\text{m}$ , WT,  $3.49 \pm 0.15$ , KO,  $2.96 \pm 0.15, p = 0.013$ ; WT,  $n = 107$  cells, KO,  $n = 122$  cells,  $n = 4$  animals per group). Two-way ANOVA,  $F_G = 10.54, p = 0.001; F_T = 27.18, p = 0.000; F_D = 92.87, p = 0.000; F_{G+T} = 34.97, p = 0.000; F_{G+D} = 1.23, p = 0.27; F_{T+D} = 23.76, p = 0.000; F_{G+T+D} = 0.92, p = 0.504$ . (F) *Left*, representative image (60x) of newborn neurons at 28 days after GFP-retroviral infection. Red, DAPI. White rectangle shows a distal dendritic region of a newborn neuron of Ca<sub>v</sub>1.3 WT mice for spine analysis. *Right*, exemplary high magnification (60x/6x-zoom) images (*top*) and 3D reconstruction images (*bottom*) of a distal dendritic region of a newborn neuron of WT and Ca<sub>v</sub>1.3 KO mice. White arrows indicate stubby spines, yellow arrows indicate mushroom spines and red arrows indicate thin spines. *Scale bar*,  $50 \mu\text{m}$  (60x),  $5 \mu\text{m}$  (60x/6x-zoom) and  $2 \mu\text{m}$  (3D image). (G) Spine density plot for each type of spines. (Thin spines, WT,  $0.82 \pm 0.07$  spines/ $\mu\text{m}$ , KO,  $0.83 \pm 0.06$  spines/ $\mu\text{m}$ ,  $p = 0.434$ ; stubby spines, WT,  $1.10 \pm 0.07$  spines/ $\mu\text{m}$ , KO,  $0.95 \pm 0.05$  spines/ $\mu\text{m}$ ,  $p = 0.064$ ; mushroom spines, WT,  $0.14 \pm 0.017$  spines/ $\mu\text{m}$ , KO,  $0.20 \pm 0.06$  spines/ $\mu\text{m}$ ,  $p = 0.409$ , WT,  $n = 28$  cells, KO,  $n = 29$  cells,  $n = 2$  animals per group). (H) *Top*, confocal images of CA3 region axonal fibers of newborn neurons at 28 days after GFP expressing retrovirus injection. Red, DAPI. *Bottom*, high magnification images of axonal boutons near CA3 pyramidal cell layer. White and yellow arrows indicate boutons and filopodia, respectively. *Insets*, 3D image of bouton and filopodia. *Scale bars*,  $50 \mu\text{m}$  (40x),  $10 \mu\text{m}$  (40x/6x-zoom),  $5 \mu\text{m}$  (*insets*). (I) Size of mossy fiber boutons (WT,  $11.52 \pm 0.47, n = 84$  boutons; KO,  $10.07 \pm 0.45, n = 70$  boutons,  $n = 3$  animals per group,  $p = 0.029$ ). (J) Total number of filopodia of axonal boutons (WT,  $3.98 \pm 0.25, n = 53$  boutons, KO,  $3.2 \pm 0.19, n = 65$  boutons,  $n = 3$  animals per group,  $p = 0.010$ ) and (K) the length of filopodia of axonal boutons (WT,  $25.99 \pm 2.02 \mu\text{m}, n = 53$  boutons, KO,  $19.16 \pm 1.29 \mu\text{m}, n = 65$  boutons,  $n = 3$  animals per group,  $p = 0.004$ ).

<https://doi.org/10.1371/journal.pone.0181138.g003>

mouse (S3E and S3F Fig). Sixth, in case of vision, results of OR test suggested that Ca<sub>v</sub>1.3 KO mouse has normal visual function (Fig 4E and 4F). These results of neurological screening along with the result of OR task suggest that deletion of Ca<sub>v</sub>1.3 would not significantly affect electrical sensitivity, locomotor activity, anxiety level, working memory performance and visual function of KO mouse, consistent with previous studies [16, 60, 62], but see McKinney et al. (2008) [18].

## Impairment of hippocampal-dependent memory tasks in Ca<sub>v</sub>1.3 KO mice

To investigate a role of Ca<sub>v</sub>1.3 in hippocampal-dependent memory tasks, Ca<sub>v</sub>1.3 KO mice were used for CFC, PA and OLR/OR learning tests. In case of recent CFC memory, it was shown that consolidation of one-trial CFC was impaired in KO mice but double-trial CFC was not [16]. In this study, both recent (Day 1) and remote ( $\geq$  Day 23) memory of CFC was investigated in KO mice (Fig 4A). The results showed that the recent CFC memory was impaired significantly in KO mice while the remote memory was not (Fig 4B). The result with KO mice suggests that lack of Ca<sub>v</sub>1.3 in mice may cause the impairment of recent CFC memory, consistent with McKinney and Murphy (2006) [16]. PA learning test showed that the remote memories at Day 42 and Day 63 of PA were impaired in KO mice by ~54% and ~80%, respectively, compared to WT mice but memory at Day 1 or 21 were normal in both groups (Fig 4C and 4D), consistent with the results of Pan et al. (2012) [38]. In case of OLR/OR tasks, OLR memory is more hippocampal-dependent than OR memory [21, 63, 64] and the recent memory of OLR task was examined because OLR task is reliable only in the recent memory task [65]. The result showed that OLR task was impaired in the recent memory performance but OR task was not in KO mice (Fig 4E and 4F). The result suggests that OLR memory processes are more sensitive to the hippocampal Ca<sub>v</sub>1.3 function.

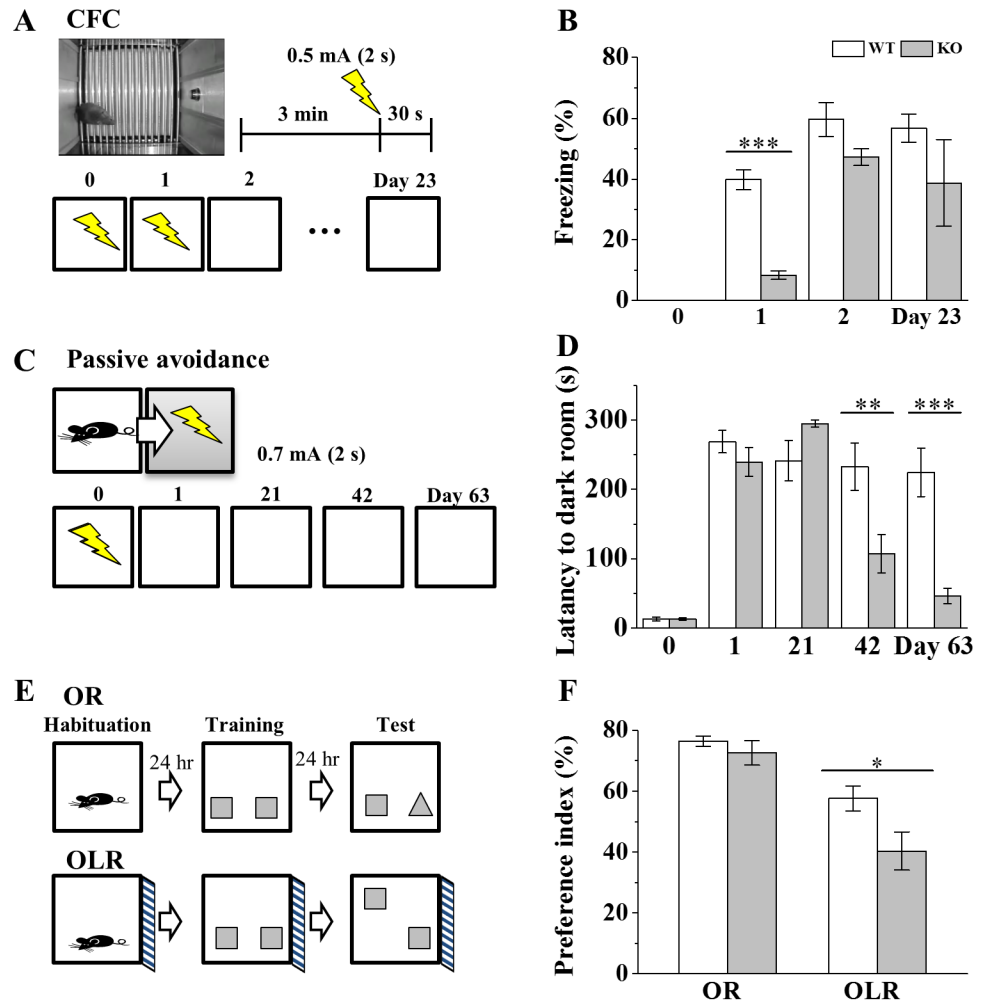


**Fig 4. Impairments of hippocampus-dependent memory tasks in  $Ca_v1.3$  KO mice.** (A) Scheme of CFC learning and memory tests. Both recent and remote CFC memories were assessed in the same chamber at Days 0, 1, 2 and 23. (B) Freezing responses of CFC memory tasks. (Day 0, WT, 0 ± 0, n = 5, KO, 0 ± 0, n = 5; Day 1, WT, 39.80 ± 3.33%, n = 15, KO, 8.39 ± 1.40%, n = 11,  $p < 0.00001$ ; Day 2, WT, 59.59 ± 5.60%, n = 13, KO, 47.18 ± 2.74%, n = 9,  $p = 0.098$ ; Day 23, WT, 56.75 ± 4.58%, n = 10, KO, 38.74 ± 14.30%, n = 6,  $p = 0.305$ ). \*, \*\*, \*\*\* indicate  $p < 0.05$ ,  $p < 0.01$ ,  $p < 0.001$ , respectively, unless otherwise mentioned. Two-way ANOVA,  $F_G = 18.24$ ,  $p = 0.000$ ;  $F_T = 17.88$ ,  $p = 0.000$ ;  $F_{G+T} = 2.31$ ,  $p = 0.106$ . (C) Scheme of PA tasks. (D) Latency of entrance to dark room of PA tasks. (Day 0, WT, 13.13 ± 2.88 s, n = 24, KO, 13.12 ± 1.75 s, n = 24,  $p = 0.990$ ; Day 1, WT, 268.89 ± 16.18 s, n = 24, KO, 239.34 ± 20.72 s, n = 24,  $p = 0.267$ ; Day 21, WT, 241.38 ± 28.90 s, n = 13, KO, 294.95 ± 5.05 s, n = 13,  $p = 0.080$ ; Day 42, WT, 232.67 ± 34.10 s, n = 9, KO, 107.22 ± 27.86 s, n = 12,  $p = 0.010$ ; Day 63, WT, 224.59 ± 34.76 s, n = 7, KO, 46.29 ± 10.71 s, n = 10,  $p = 0.000$ ). Two-way ANOVA,  $F_G = 2.45$ ,  $p = 0.12$ ;  $F_T = 17.47$ ,  $p = 0.00$ ;  $F_{G+T} = 2.33$ ,  $p = 0.08$ . (E) Schemes of OR and OLR tasks. (F) Preference index measurement of OR/OLR tasks. (OR task: WT, 76.41 ± 1.66%, n = 11, KO, 72.54 ± 4.0%, n = 9,  $p = 0.339$ ; OLR task: WT, 55.19 ± 4.04%, n = 11, KO, 42.89 ± 4.13%, n = 9,  $p = 0.048$ ).

<https://doi.org/10.1371/journal.pone.0181138.g004>

### Impairment of both recent and remote CFC memories in dorsal hippocampal AAV- $Ca_v1.3$ KD mice

Results of KO mice study indicate that  $Ca_v1.3$  is necessary for the memory of hippocampal-dependent learning tasks but they cannot tell the type and location of cells involved. To identify regions of hippocampus where neuronal  $Ca_v1.3$  plays a role in CFC learning and memory, GFP-AAV containing  $Ca_v1.3$  KD shRNA and control GFP-AAV were made (S4A–S4C Fig)

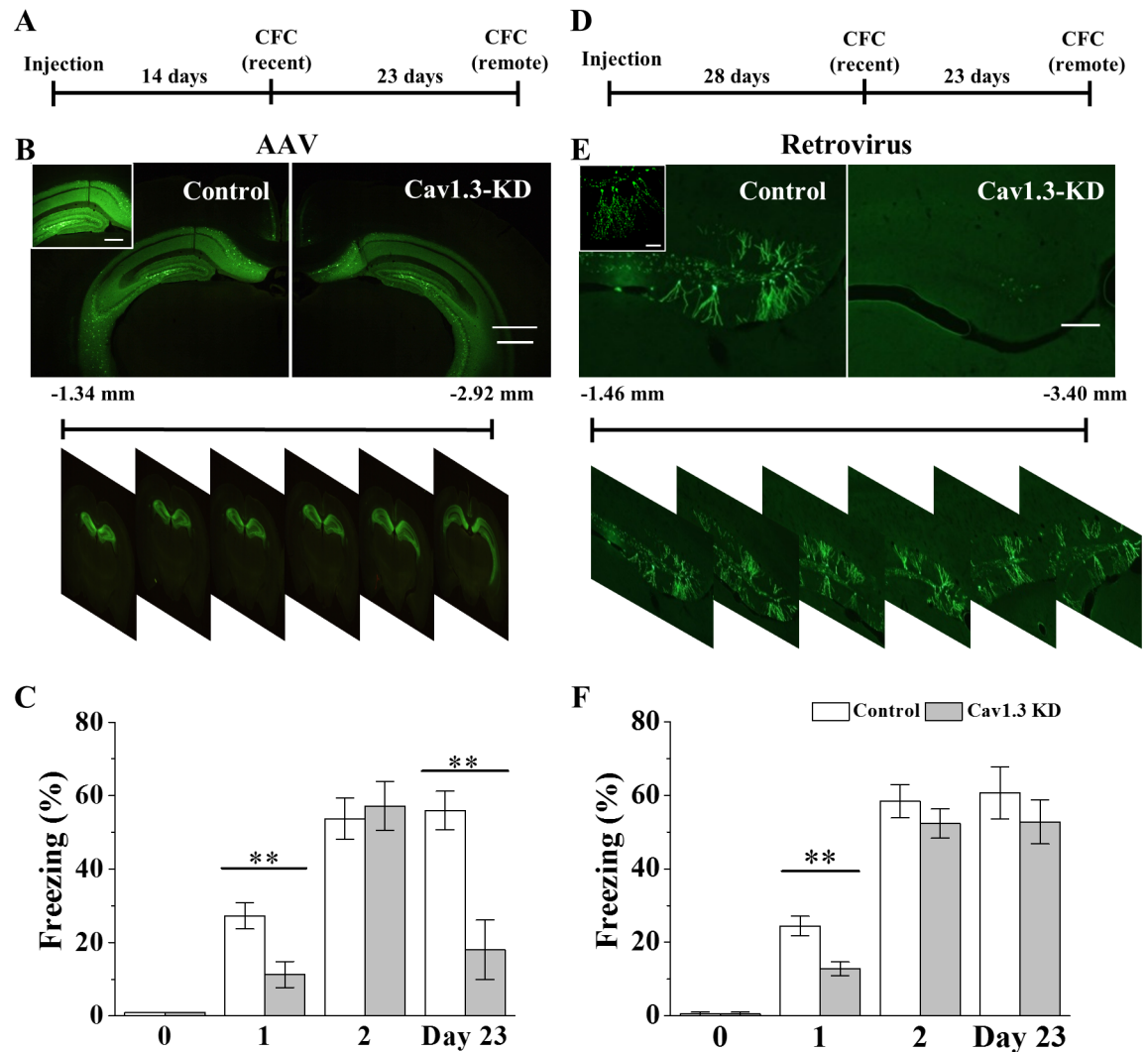


**Fig 5. Effects of AAV- and retroviral-Ca<sub>v</sub>1.3 KD on both recent and remote memories of CFC.** (A) Experimental scheme of recent and remote memory tests of CFC using AAV mediated Ca<sub>v</sub>1.3 KD in dorsal hippocampus. (B) *Top*, Representative images of GFP expression of AAV-Ca<sub>v</sub>1.3 KD cells in dorsal hippocampus. *Scale bars*, 500 μm and 200 μm (*insets*). *Bottom*, representative images of expression of GFP (+) AAV-Ca<sub>v</sub>1.3 KD control into the dorsal hippocampus of F1 mouse at 2 week of infection. (C) Freezing responses in AAV-Ca<sub>v</sub>1.3 KD and control mice. (Day 0, Control, 0 ± 0, n = 5, KD, 0 ± 0, n = 5; Day 1, Control, 27.25 ± 3.57%, n = 19, KD, 11.31 ± 3.55%, n = 17, *p* = 0.003; Day 2, Control, 53.74 ± 5.58%, n = 8, KD, 57.13 ± 6.65%, n = 7, *p* = 0.697; Day 23, Control, 55.96 ± 5.20%, n = 8, KD, 18.00 ± 8.11%, n = 7, *p* = 0.001). \*\* indicates *p* < 0.01. (D) Experimental scheme of recent and remote memory tests of CFC using retroviral mediated Ca<sub>v</sub>1.3 KD in dorsal hippocampus. Two-way ANOVA, *F*<sub>G</sub> = 15.09, *p* = 0.000; *F*<sub>T</sub> = 27.49, *p* = 0.000; *F*<sub>G+T</sub> = 6.12, *p* = 0.004. (E) *Top*, Representative images of GFP expression of retroviral-Ca<sub>v</sub>1.3 KD cells in DG of dorsal hippocampus at 28 days after infection. *Scale bars*, 200 μm and 50 μm (*insets*). *Bottom*, representative images of expression of GFP (+) retrovirus-Ca<sub>v</sub>1.3 KD control into the dorsal hippocampus of F1 mouse at 4 week of infection. (F) Freezing responses in retroviral-Ca<sub>v</sub>1.3 KD and control mice. (Day 0, Control, 0 ± 0, n = 5, KD, 0 ± 0, n = 5; Day 1, Control, 24.46 ± 2.63%, n = 14, KD, 12.80 ± 1.88%, n = 15, *p* = 0.003; Day 2, Control, 58.40 ± 4.54%, n = 14, KD, 52.33 ± 3.96%, n = 15, *p* = 0.321; Day 23, Control, 60.66 ± 7.09%, n = 9, KD, 52.78 ± 6.00%, n = 9, *p* = 0.409). Two-way ANOVA, *F*<sub>G</sub> = 4.33, *p* = 0.041; *F*<sub>T</sub> = 32.07, *p* = 0.000; *F*<sub>G+T</sub> = 0.14, *p* = 0.866.

<https://doi.org/10.1371/journal.pone.0181138.g005>

and injected into DG area of dorsal hippocampus (Fig 5B; S4D and S5A–S5C Figs). The results showed that KD of Ca<sub>v</sub>1.3 of infected neurons in dorsal hippocampus reduced both recent and remote memories of CFC by ~59% and ~68%, respectively (Fig 5C). Compared with KO mice data, significant suppression of remote CFC memory was observed in mice where KD



occurred in dorsal hippocampal area only. Interestingly, CFC memory of intermediate period (Day 2) was normal in KD mice [16], further suggesting that the contribution of Ca<sub>v</sub>1.3 or the mechanism of CFC memory process might change dynamically along time [66]. The results suggest that Ca<sub>v</sub>1.3 in mature neurons of dorsal hippocampus is important for both recent and remote memories of CFC learning and Ca<sub>v</sub>1.3 activity from some group of neurons is enough for maintaining these CFC memories. Moreover, KD of Ca<sub>v</sub>1.3 in ventral hippocampal area by shRNA AAV did not impair the recent CFC memory (S4E and S4F Fig), suggesting that CFC learning and memory might use neuronal circuits of dorsal hippocampus mainly [67]. Another possibility is that the current KD method cannot affect all the ventral hippocampal neurons which are critically involved in CFC memory.

### Impairment of recent CFC memory in dorsal hippocampal retroviral-Ca<sub>v</sub>1.3 KD mice

The relationship between neurogenesis and memory tasks seems complex. In PA task, Pan et al. (2012) [38] showed that the remote PA memory was more dependent upon adult hippocampal neurogenesis than the recent memory. In case of OR/OLR tasks, OLR memory was dependent on adult hippocampal neurogenesis but OR memory was not [21, 63]. In spatial memory, both recent and remote memories were inhibited when adult hippocampal neurogenesis was impaired [21, 38, 68]. Since Ca<sub>v</sub>1.3 KO mouse has reduced survival rate of newborn neurons, it is plausible that the inhibitory effect on either recent memories of CFC and OLR or remote PA memory might be also due to the impaired neurogenesis in KO mice. To test this idea on CFC memory task, retrovirus-mediated KD method was adopted for gene regulation in proliferating neurons [36, 69]. To identify a role of Ca<sub>v</sub>1.3 in adult newborn neurons, GFP-Ca<sub>v</sub>1.3 shRNA-retrovirus and KD control GFP-retrovirus were generated and injected into DG area of dorsal hippocampus (Fig 5D; S6A and S6B Fig). The results showed that recent CFC memory was impaired in KD mice but remote CFC memory was not (Fig 5F). In KD mouse, bright GFP (+) neurons were rarely detected at ≥ 4 week of infection (≥ 10 animals). It is possible that infected newborn neurons might die out during the infection period, further convincing the positive effect of Ca<sub>v</sub>1.3 on survival of newborn neurons during that period (Fig 1). The results suggest that Ca<sub>v</sub>1.3 of newborn neurons in DG of dorsal hippocampus plays a critical role in the recent memory of CFC learning, possibly by helping the survival of newborn neurons, and some newborn neurons of dorsal hippocampal area might be enough for performing the CFC memory task.

### Discussion

It has been reported that Ca<sub>v</sub>1.3 may regulate survival of adult newborn neurons and hippocampal-dependent memory such as CFC [16, 20]. However, it is unclear how Ca<sub>v</sub>1.3 is involved in adult neurogenesis process and what regional neurons of hippocampus are sufficiently related with hippocampal-dependent learning & memory tasks. This study focused on roles of Ca<sub>v</sub>1.3 in the development of newborn neurons using KO mice and on the regional role of Ca<sub>v</sub>1.3 within hippocampus in learning & memory tasks using KD strategy. Functions of Ca<sub>v</sub>1.3 of mature or immature neurons in learning & memory were tried to be differentiated with AAV- vs retroviral KD methods. We show that Ca<sub>v</sub>1.3 plays a role for proper developments of dendrites, MFBs and filopodia of MFBs of adult newborn neurons during maturation and confirm the reduction of survival of newborn neurons in Ca<sub>v</sub>1.3 KO mice. We further show that various hippocampal-dependent memory tasks are impaired in KO mice and AAV KD of Ca<sub>v</sub>1.3 only in some of dorsal hippocampal neurons seems enough to impair CFC memory. Meanwhile, AAV KD in ventral hippocampal area has little effect on CFC memory.

Moreover, retroviral KD mice study reveals a function of Ca<sub>v</sub>1.3 of dorsal hippocampal newborn cells in the recent CFC memory.

## Endogenous expression of Ca<sub>v</sub>1.3 during development of newborn neuron overlaps with the period of survival of newborn cells

Ca<sub>v</sub>1.3 is expressed in hippocampus [1, 10, 70]. LTCC blockers have reduced the survival and differentiation of late stage newborn neurons *in vitro* and *in vivo* [30, 31, 33, 71]. Recent Ca<sub>v</sub>1.3 KO mouse studies showed the reduction of survival of newborn neurons in adult hippocampus [20, 34]. Co-expressions of Ca<sub>v</sub>1.3 with neurogenesis stage makers such as nestin, PCNA, DCX, NeuN and GFAP have been shown in adult hippocampus [20]. However, it is still unclear how Ca<sub>v</sub>1.3 of newborn neurons is regulated and what functions it is related with. In this study, we find that Ca<sub>v</sub>1.3 expression in adult newborn cells starts to increase during maturation stage ( $\geq$  day 14) of development (Fig 1C and 1D), which coincides in general with the fate decision stage of newborn cells [72]. Moreover, we further show that the reduction of survival of newborn neurons occurs mostly around 28 days after mitosis in both WT and KO mice (Fig 2A–2D), which overlaps with the time when Ca<sub>v</sub>1.3 expression in newborn neurons becomes near the level of mature neurons (Fig 1D). In addition, the reduction of BrdU (+) cells at day 28 even in WT mouse suggests that Ca<sub>v</sub>1.3 is only a part of endogenous survival process of newborn neurons. It will be interesting to know whether overexpression or faster expression of Ca<sub>v</sub>1.3 in newborn neurons during early developmental period could inhibit or slow down the reduction of survival rate. Recently Kruger et al. (2017) developed a Ca<sub>v</sub>1.3 overexpressing transgenic mouse for normal aging model, which can be used for testing these possibilities [73]. In summary, the correlation of the period of enhanced Ca<sub>v</sub>1.3 expression in WT mice with the reduction of survival of adult newborn neurons in KO mice suggests an endogenous function of Ca<sub>v</sub>1.3 in the survival process of newborn neurons. For comparison, Ca<sub>v</sub>1.2 forebrain KO also showed the reduction of survival of newborn neurons [38]. The exact functional difference of Ca<sub>v</sub>1.2 and Ca<sub>v</sub>1.3 in the newborn neuron survival process remains to be studied.

## Ca<sub>v</sub>1.3 is necessary for the development of dendrites, MFBs and MFB filopodia of newborn neurons and for their survival

Newborn neurons derived from NSCs of DG need to develop proper dendrites and axonal terminals for synaptogenesis, while avoiding cellular death pathways, and thereby timely synaptic integration into preexisting neural networks, which is necessary for the functional maturation and survival [53]. LTCCs have been implicated in the neurite outgrowth of immature neuronal cell lines and cultured hippocampal or cortical neurons [74–80]. However it is unclear how LTCC isoforms are involved during neuronal development. Ca<sub>v</sub>1.2 is observed in pioneer axons of developing forebrain [81] and Ca<sub>v</sub>1.3 KO mice shows the reduction of axon arbor morphology in auditory brainstem at P10–12 [82]. We find that the development of MFB filopodia near CA3 as well as the growth of dendrites of DG newborn neurons is impaired in Ca<sub>v</sub>1.3 KO mice (Fig 3). Lesser growth of dendrites and axonal filopodia might result in the less formation of functional synapses of newborn neurons when it is time for synaptic integration to occur.

The positive relationship between neuronal outgrowth and survival of newborn neurons has been suggested. Impairments of both survival and neurite outgrowth of newborn neurons were observed [83–86] and enhancement of neurite outgrowth of newborn neurons was associated with their survival *in vivo* [87]. Furthermore, the correlation of reduction of survival and spine density in adult newborn neurons *in vivo* was also shown [84, 88, 89]. When spines

get mature, it changes morphology from thin filopodia to stubby to mushroom shape, reflecting a maturation stage or functional difference [46]. The result shows that during the early stage of development, most spines of newborn neurons are either thin filopodia or stubby type and mushroom type is a few, which is consistent with the expectation when functional synapses have not yet been actively formed. Our result suggests that Ca<sub>v</sub>1.3 might be involved in the stability or formation of stubby spines and Ca<sub>v</sub>1.3 deletion would reduce the functional synapse formation and survival of newborn neurons, resulting in the impairment of hippocampal-dependent learning and memory tasks.

The relationship between the survival of adult newborn neurons and the volume/area of DG has been controversial [20, 34]. Marschallinger et al. (2015) has described the correlation of the reduction of DG volume and the survival of adult neurogenesis in Ca<sub>v</sub>1.3 KO mice [20]. Meanwhile, our results show that areas of DG GCL as well as DG were not changed though newborn cell survival is reduced in Ca<sub>v</sub>1.3 KO mice. This inconsistency may be caused by difference of age of animals or quantification methods. Recently, Lee et al. (2016) [34] have reported no change of DG GCL thickness in forebrain Ca<sub>v</sub>1.2 cKO mice that exhibit the reduction of survival of adult newborn neurons. The clarification of the relationship between the total DG cell number and the neurogenesis activity remains to be studied along the age of mouse.

### Ca<sub>v</sub>1.3 in mature or immature neurons of dorsal DG regions plays differential roles in CFC memory processes

Role of LTCCs in the consolidation of CFC has been reported using pharmacological and genetic methods [11, 13, 16, 90] and DG-CA3 regions of dorsal hippocampus are suggested for their involvement in contextual memory using lesion or gene deletion methods [66, 91]. McKinney et al. (2006, 2009) has described significant impairment in the consolidation of recent CFC memory without impairment in the extinction of Ca<sub>v</sub>1.3 KO mice [3, 16]. Studies of conventional KO mice did not tell what brain region, such as dorsal vs ventral hippocampus, is important for the memory of CFC. Some electrolytic and pharmacological lesion studies suggest dorsal hippocampus as a functional region for CFC [92–96] and others relate ventral hippocampus with CFC memory [97–99]. In this study, we showed virus-mediated localized effect of Ca<sub>v</sub>1.3 KD on CFC memory for the first time. The impairment of both recent and remote memories of CFC learning was observed in mice where AAV-Ca<sub>v</sub>1.3 KD occurs in DG-CA3 regions of dorsal hippocampus (Fig 5A; S4D Fig). On the contrary, the recent CFC memory was normal when AAV KD occurs in ventral hippocampal area (S4E and S4F Fig), suggesting a dominant role of Ca<sub>v</sub>1.3 in the dorsal hippocampal circuitry in the recent CFC memory process.

Regarding role of newborn neurons in learning and memory process, it was shown that enhancement of hippocampal neurogenesis improved the learning and memory tasks such as CFC, OR, PA and water-maze [23, 100, 101]. And ablation of hippocampal neurogenesis using x-ray irradiation or pharmacological or transgenic methods impaired CFC learning [24–26, 102]. It has been suggested that Ca<sub>v</sub>1.3 and adult neurogenesis are related with OLR memory [20] and 4 to 6 week old newborn neurons are involved in CFC and OR tasks using x-ray irradiation [28]. Here, by applying retrovirus-mediated Ca<sub>v</sub>1.3 KD in dorsal hippocampal area for the first time, we revealed the impairment of recent CFC memory when KD was maintained for 4 weeks (Fig 5F).

Our results suggest that Ca<sub>v</sub>1.3 channel of adult dorsal hippocampal neurons, either immature or mature, has endogenous functions in CFC memory process. Relating to Ca<sub>v</sub>1.2, deletion in forebrain Ca<sub>v</sub>1.2 had no effect on the consolidation and extinction of CFC [18] but was

critical on the remote memory of water-maze [17]. Therefore, it seems that both Ca<sub>v</sub>1.2 and Ca<sub>v</sub>1.3 do have differential roles depending on the kind of learning and memory task.

### Role of Ca<sub>v</sub>1.3 in PA, OR and OLR task

LTCCs antagonists have produced controversial results about the role of LTCCs in PA task. LTCC blockers such as verapamil or nimodipine induced either impairment or enhancement of PA [103–106]. We find that KD of Ca<sub>v</sub>1.3 in dorsal hippocampal neurons inhibits the remote PA memory. In case of OR and OLR tasks, our results suggest that Ca<sub>v</sub>1.3 has a role in the recent OLR memory but not in OR task, consistent with Marschallinger et al. (2015) [20]. However, Pan et al. (2012) has described that the inhibition of adult neurogenesis induced by deletion of ERK5 is associated with the impairment in the memory at 48 hours after training of OR task [38]. These results indicate that there might be diverse mechanisms for OR or OLR memory process in terms of involvement of neurogenesis and type of LTCC isoforms or depending on the memory duration.

In this study, we have shown that Ca<sub>v</sub>1.3 in dorsal hippocampal neurons is involved in the development and survival of newborn neurons and in hippocampal-dependent learning and memory tasks. However, the mechanism of how Ca<sub>v</sub>1.3 contributes to the survival or death of newborn cells during development remains to be studied. Our results do not tell whether the effect of Ca<sub>v</sub>1.3 removal on the survival and development of newborn cells is cell-autonomous effect or not. Therefore, it will be interesting to know whether Ca<sub>v</sub>1.3 mediated Ca<sup>2+</sup>-dependent survival of newborn neurons is cell-autonomous process or not. Activity-dependent modulation of adult hippocampal neurogenesis suggests that extrinsic factors such as GABA or neuropeptides as well as synaptic activity might also be involved in the survival of newborn neurons [30, 107, 108]. Newborn neurons are derived from NSCs which are originated from glial cells [109, 110]. As a supplier of extrinsic niche environments, glial cells are known to release neurotransmitters such as glutamate and GABA as well as diverse cytokines and nitric oxide through intracellular Ca<sup>2+</sup>-dependent or—independent ways [111]. Since Ca<sub>v</sub>1.3 is expressed in nestin (+) NSCs and Ca<sub>v</sub>1.3 deletion leads to a decrease of hippocampal neurogenesis and of GFAP (+) area in 3-month old mice, it will be important to further clarify the role of Ca<sub>v</sub>1.3 during transitions from glia-like NSCs to newborn neurons to mature neurons.

### Supporting information

#### **S1 Fig. Characterization of Ca<sub>v</sub>1.3 KO mice.**

(TIF)

#### **S2 Fig. Expression of Ca<sub>v</sub>1.3 and DCX of dorsal hippocampus in Ca<sub>v</sub>1.3 WT and KO mice.**

(TIF)

#### **S3 Fig. Neurological screening tests in Ca<sub>v</sub>1.3 KO mice.**

(TIF)

#### **S4 Fig. Characterization of AAV-mediated Ca<sub>v</sub>1.3 KD *in vitro* and *in vivo*.**

(TIF)

#### **S5 Fig. Comparison of GFP expressions at dorsal and ventral hippocampus mediated by AAV-Ca<sub>v</sub>1.3 KD injections, respectively.**

(TIF)

#### **S6 Fig. Characterization of retrovirus-mediated GFP (+) Ca<sub>v</sub>1.3 KD *in vitro* and *in vivo*.**

(TIF)

**S1 File. A role of Cav1.3 channels in behavior for POne-SI-v11.**  
(DOCX)

**S2 File. NC3Rs ARRIVE guidelines checklist (fillable)-chkim-v1.**  
(PDF)

## Acknowledgments

We thank Drs. R. J. DiLeone, H. S. Shin, H. Song and F. H. Gage for their plasmids. We also thank D.-H. Choi, S. Song, and J. Lee for assisting with statistical analysis and data quantification.

## Author Contributions

**Conceptualization:** Chong-Hyun Kim.

**Data curation:** Su-Hyun Kim, Ye-Ryoung Park, Boyoung Lee, Byungil Choi.

**Formal analysis:** Su-Hyun Kim.

**Funding acquisition:** Chong-Hyun Kim.

**Investigation:** Chong-Hyun Kim.

**Methodology:** Ye-Ryoung Park, Byungil Choi, Hyun Kim.

**Project administration:** Chong-Hyun Kim.

**Resources:** Boyoung Lee, Byungil Choi, Hyun Kim, Chong-Hyun Kim.

**Supervision:** Chong-Hyun Kim.

**Validation:** Hyun Kim, Chong-Hyun Kim.

**Visualization:** Su-Hyun Kim.

**Writing – original draft:** Su-Hyun Kim, Chong-Hyun Kim.

**Writing – review & editing:** Chong-Hyun Kim.

## References

1. Casamassima F, Hay AC, Benedetti A, Lattanzi L, Cassano GB, Perlis RH. L-type calcium channels and psychiatric disorders: A brief review. *Am J Med Genet B Neuropsychiatr Genet.* 2010; 153b(8):1373–90. Epub 2010/10/05. <https://doi.org/10.1002/ajmg.b.31122> PMID: 20886543.
2. Leitch B, Szostek A, Lin R, Shevtsova O. Subcellular distribution of L-type calcium channel subtypes in rat hippocampal neurons. *Neuroscience.* 2009; 164(2):641–57. <https://doi.org/10.1016/j.neuroscience.2009.08.006> PMID: 19665524.
3. McKinney BC, Sze W, Lee B, Murphy GG. Impaired long-term potentiation and enhanced neuronal excitability in the amygdala of Ca(V)1.3 knockout mice. *Neurobiol Learn Mem.* 2009; 92(4):519–28. <https://doi.org/10.1016/j.nlm.2009.06.012> PMID: 19595780;
4. Liu Y, Harding M, Pittman A, Dore J, Striessnig J, Rajadhyaksha A, et al. Cav1.2 and Cav1.3 L-type calcium channels regulate dopaminergic firing activity in the mouse ventral tegmental area. *J Neurophysiol.* 2014; 112(5):1119–30. <https://doi.org/10.1152/jn.00757.2013> PMID: 24848473;
5. Zhang H, Fu Y, Altier C, Platzer J, Surmeier DJ, Bezprozvanny I. Ca1.2 and CaV1.3 neuronal L-type calcium channels: differential targeting and signaling to pCREB. *Eur J Neurosci.* 2006; 23(9):2297–310. <https://doi.org/10.1111/j.1460-9568.2006.04734.x> PMID: 16706838;
6. D'Arco M, Dolphin AC. L-type calcium channels: on the fast track to nuclear signaling. *Sci Signal.* 2012; 5(237):pe34. <https://doi.org/10.1126/scisignal.2003355> PMID: 22894834.
7. Kapur A, Yeckel MF, Gray R, Johnston D. L-Type calcium channels are required for one form of hippocampal mossy fiber LTP. *J Neurophysiol.* 1998; 79(4):2181–90. PMID: 9535977;



8. Jensen K, Mody I. L-type Ca<sup>2+</sup> channel-mediated short-term plasticity of GABAergic synapses. *Nat Neurosci*. 2001; 4(10):975–6. <https://doi.org/10.1038/nn722> PMID: 11547336.
9. Hulme SR, Connelly WM. L-type calcium channel-dependent inhibitory plasticity in the thalamus. *J Neurophysiol*. 2014; 112(9):2037–9. <https://doi.org/10.1152/jn.00918.2013> PMID: 24623510;
10. Berger SM, Bartsch D. The role of L-type voltage-gated calcium channels Cav1.2 and Cav1.3 in normal and pathological brain function. *Cell Tissue Res*. 2014; 357(2):463–76. Epub 2014/07/06. <https://doi.org/10.1007/s00441-014-1936-3> PMID: 24996399.
11. Bauer EP, Schafe GE, LeDoux JE. NMDA Receptors and L-Type Voltage-Gated Calcium Channels Contribute to Long-Term Potentiation and Different Components of Fear Memory Formation in the Lateral Amygdala. *The Journal of Neuroscience*. 2002; 22(12):5239–49. PMID: 12077219
12. Cain CK, Blouin AM, Barad M. L-type voltage-gated calcium channels are required for extinction, but not for acquisition or expression, of conditional fear in mice. *J Neurosci*. 2002; 22(20):9113–21. Epub 2002/10/22. PMID: 12388619.
13. Cain CK, Godsil BP, Jami S, Barad M. The L-type calcium channel blocker nifedipine impairs extinction, but not reduced contingency effects, in mice. *Learn Mem*. 2005; 12(3):277–84. Epub 2005/06/03. <https://doi.org/10.1101/lm.88805> PMID: 15930506;
14. Striessnig J, Pinggera A, Kaur G, Bock G, Tuluc P. L-type Ca<sup>2+</sup> channels in heart and brain. *Wiley Interdiscip Rev Membr Transp Signal*. 2014; 3(2):15–38. <https://doi.org/10.1002/wmts.102> PMID: 24683526;
15. Moosmang S, Haider N, Klugbauer N, Adelsberger H, Langwieser N, Muller J, et al. Role of hippocampal Cav1.2 Ca<sup>2+</sup> channels in NMDA receptor-independent synaptic plasticity and spatial memory. *J Neurosci*. 2005; 25(43):9883–92. <https://doi.org/10.1523/JNEUROSCI.1531-05.2005> PMID: 16251435.
16. McKinney BC, Murphy GG. The L-Type voltage-gated calcium channel Cav1.3 mediates consolidation, but not extinction, of contextually conditioned fear in mice. *Learn Mem*. 2006; 13(5):584–9. <https://doi.org/10.1101/lm.279006> PMID: 17015855;
17. White JA, McKinney BC, John MC, Powers PA, Kamp TJ, Murphy GG. Conditional forebrain deletion of the L-type calcium channel Ca V 1.2 disrupts remote spatial memories in mice. *Learn Mem*. 2008; 15(1):1–5. <https://doi.org/10.1101/lm.773208> PMID: 18174367.
18. McKinney BC, Sze W, White JA, Murphy GG. L-type voltage-gated calcium channels in conditioned fear: a genetic and pharmacological analysis. *Learn Mem*. 2008; 15(5):326–34. <https://doi.org/10.1101/lm.893808> PMID: 18441291;
19. Jeon D, Kim S, Chetana M, Jo D, Ruley HE, Lin SY, et al. Observational fear learning involves affective pain system and Cav1.2 Ca<sup>2+</sup> channels in ACC. *Nat Neurosci*. 2010; 13(4):482–8. <https://doi.org/10.1038/nn.2504> PMID: 20190743;
20. Marschallinger J, Sah A, Schmuckermaier C, Unger M, Rotheneichner P, Kharitonova M, et al. The L-type calcium channel Cav1.3 is required for proper hippocampal neurogenesis and cognitive functions. *Cell Calcium*. 2015; 58(6):606–16. <https://doi.org/10.1016/j.ceca.2015.09.007> PMID: 26459417.
21. Goodman T, Trouche S, Massou I, Verret L, Zerwas M, Roulet P, et al. Young hippocampal neurons are critical for recent and remote spatial memory in adult mice. *Neuroscience*. 2010; 171(3):769–78. <https://doi.org/10.1016/j.neuroscience.2010.09.047> PMID: 20883747.
22. Aasebo IE, Blankvoort S, Tashiro A. Critical maturational period of new neurons in adult dentate gyrus for their involvement in memory formation. *Eur J Neurosci*. 2011; 33(6):1094–100. <https://doi.org/10.1111/j.1460-9568.2011.07608.x> PMID: 21395853.
23. Yau SY, Li A, So KF. Involvement of Adult Hippocampal Neurogenesis in Learning and Forgetting. *Neural Plast*. 2015; 2015:717958. Epub 2015/09/18. <https://doi.org/10.1155/2015/717958> PMID: 26380120;
24. Saxe MD, Battaglia F, Wang JW, Malleret G, David DJ, Monckton JE, et al. Ablation of hippocampal neurogenesis impairs contextual fear conditioning and synaptic plasticity in the dentate gyrus. *Proc Natl Acad Sci U S A*. 2006; 103(46):17501–6. <https://doi.org/10.1073/pnas.0607207103> PMID: 17088541;
25. Ko HG, Jang DJ, Son J, Kwak C, Choi JH, Ji YH, et al. Effect of ablated hippocampal neurogenesis on the formation and extinction of contextual fear memory. *Mol Brain*. 2009; 2:1. <https://doi.org/10.1186/1756-6606-2-1> PMID: 19138433;
26. Hernandez-Rabaza V, Llorens-Martin M, Velazquez-Sanchez C, Ferragud A, Arcusa A, Gumus HG, et al. Inhibition of adult hippocampal neurogenesis disrupts contextual learning but spares spatial working memory, long-term conditional rule retention and spatial reversal. *Neuroscience*. 2009; 159(1):59–68. <https://doi.org/10.1016/j.neuroscience.2008.11.054> PMID: 19138728.

27. Drew MR, Denny CA, Hen R. Arrest of adult hippocampal neurogenesis in mice impairs single- but not multiple-trial contextual fear conditioning. *Behav Neurosci*. 2010; 124(4):446–54. <https://doi.org/10.1037/a0020081> PMID: 20695644;
28. Denny CA, Burghardt NS, Schachter DM, Hen R, Drew MR. 4- to 6-week-old adult-born hippocampal neurons influence novelty-evoked exploration and contextual fear conditioning. *Hippocampus*. 2012; 22(5):1188–201. <https://doi.org/10.1002/hipo.20964> PMID: 21739523;
29. Gross CT, Canteras NS. The many paths to fear. *Nat Rev Neurosci*. 2012; 13(9):651–8. <https://doi.org/10.1038/nrn3301> PMID: 22850830.
30. Deisseroth K, Singla S, Toda H, Monje M, Palmer TD, Malenka RC. Excitation-neurogenesis coupling in adult neural stem/progenitor cells. *Neuron*. 2004; 42(4):535–52. Epub 2004/05/26. PMID: 15157417.
31. D'Ascenzo M, Piacentini R, Casalbore P, Budoni M, Pallini R, Azzena GB, et al. Role of L-type Ca<sup>2+</sup> channels in neural stem/progenitor cell differentiation. *Eur J Neurosci*. 2006; 23(4):935–44. <https://doi.org/10.1111/j.1460-9568.2006.04628.x> PMID: 16519658.
32. Lee H, Lee D, Park CH, Ho WK, Lee SH. GABA mediates the network activity-dependent facilitation of axonal outgrowth from the newborn granule cells in the early postnatal rat hippocampus. *Eur J Neurosci*. 2012; 36(6):2743–52. <https://doi.org/10.1111/j.1460-9568.2012.08192.x> PMID: 22780325.
33. Teh DB, Ishizuka T, Yawo H. Regulation of later neurogenic stages of adult-derived neural stem/progenitor cells by L-type Ca<sup>2+</sup> channels. *Dev Growth Differ*. 2014; 56(8):583–94. <https://doi.org/10.1111/dgd.12158> PMID: 25283796.
34. Lee AS, De Jesus-Cortes H, Kabir ZD, Knobbe W, Orr M, Burgdorf C, et al. The Neuropsychiatric Disease-Associated Gene *cacna1c* Mediates Survival of Young Hippocampal Neurons. *eNeuro*. 2016; 3(2). <https://doi.org/10.1523/ENEURO.0006-16.2016> PMID: 27066530;
35. Platzer J, Engel J, Schrott-Fischer A, Stephan K, Bova S, Chen H, et al. Congenital deafness and sinoatrial node dysfunction in mice lacking class D L-type Ca<sup>2+</sup> channels. *Cell*. 2000; 102(1):89–97. PMID: 10929716.
36. Zhao C, Teng EM, Summers RG Jr., Ming GL, Gage FH. Distinct morphological stages of dentate granule neuron maturation in the adult mouse hippocampus. *J Neurosci*. 2006; 26(1):3–11. <https://doi.org/10.1523/JNEUROSCI.3648-05.2006> PMID: 16399667.
37. Rodriguez A, Ehlenberger DB, Dickstein DL, Hof PR, Wearne SL. Automated three-dimensional detection and shape classification of dendritic spines from fluorescence microscopy images. *PLoS One*. 2008; 3(4):e1997. <https://doi.org/10.1371/journal.pone.0001997> PMID: 18431482;
38. Pan YW, Chan GC, Kuo CT, Storm DR, Xia Z. Inhibition of adult neurogenesis by inducible and targeted deletion of ERK5 mitogen-activated protein kinase specifically in adult neurogenic regions impairs contextual fear extinction and remote fear memory. *J Neurosci*. 2012; 32(19):6444–55. <https://doi.org/10.1523/JNEUROSCI.6076-11.2012> PMID: 22573667;
39. Hell JW, Westenbroek RE, Warner C, Ahljianian MK, Prystay W, Gilbert MM, et al. Identification and differential subcellular localization of the neuronal class C and class D L-type calcium channel alpha 1 subunits. *J Cell Biol*. 1993; 123(4):949–62. Epub 1993/11/01. PMID: 8227151;
40. Xu JH, Yang ZB, Wang H, Tang FR. Co-localization of L-type voltage dependent calcium channel alpha 1D subunit (Ca(v)1.3) and calbindin (CB) in the mouse central nervous system. *Neurosci Lett*. 2014; 561:80–5. <https://doi.org/10.1016/j.neulet.2013.12.057> PMID: 24394909.
41. Veng LM, Browning MD. Regionally selective alterations in expression of the alpha(1D) subunit (Ca(v)1.3) of L-type calcium channels in the hippocampus of aged rats. *Brain Res Mol Brain Res*. 2002; 107(2):120–7. Epub 2002/11/12. PMID: 12425941.
42. Noto B, Klempin F, Alenina N, Bader M, Fink H, Sander SE. Increased adult neurogenesis in mice with a permanent overexpression of the postsynaptic 5-HT1A receptor. *Neurosci Lett*. 2016; 633:246–51. Epub 2016/10/22. <https://doi.org/10.1016/j.neulet.2016.09.051> PMID: 27693660.
43. Tozuka Y, Fukuda S, Namba T, Seki T, Hisatsune T. GABAergic excitation promotes neuronal differentiation in adult hippocampal progenitor cells. *Neuron*. 2005; 47(6):803–15. <https://doi.org/10.1016/j.neuron.2005.08.023> PMID: 16157276.
44. Shelly M, Lim BK, Cancedda L, Heilshorn SC, Gao H, Poo MM. Local and long-range reciprocal regulation of cAMP and cGMP in axon/dendrite formation. *Science*. 2010; 327(5965):547–52. Epub 2010/01/30. <https://doi.org/10.1126/science.1179735> PMID: 20110498.
45. Schindelin J, Arganda-Carreras I, Frise E, Kaynig V, Longair M, Pietzsch T, et al. Fiji: an open-source platform for biological-image analysis. *Nat Methods*. 2012; 9(7):676–82. Epub 2012/06/30. <https://doi.org/10.1038/nmeth.2019> PMID: 22743772;
46. Ethell IM, Pasquale EB. Molecular mechanisms of dendritic spine development and remodeling. *Progress in Neurobiology*. 2005; 75(3):161–205. <http://dx.doi.org/10.1016/j.pneurobio.2005.02.003> PMID: 15882774

47. Hoogland TM, Saggau P. Facilitation of L-type Ca<sup>2+</sup> channels in dendritic spines by activation of beta<sub>2</sub> adrenergic receptors. *J Neurosci*. 2004; 24(39):8416–27. Epub 2004/10/01. <https://doi.org/10.1523/JNEUROSCI.1677-04.2004> PMID: 15456814.
48. Higley MJ, Sabatini BL. Calcium signaling in dendritic spines. *Cold Spring Harb Perspect Biol*. 2012; 4(4):a005686. Epub 2012/02/18. <https://doi.org/10.1101/cshperspect.a005686> PMID: 22338091;
49. Stanika R, Campiglio M, Pinggera A, Lee A, Striessnig J, Flucher BE, et al. Splice variants of the CaV1.3 L-type calcium channel regulate dendritic spine morphology. *Sci Rep*. 2016; 6:34528. Epub 2016/10/07. <https://doi.org/10.1038/srep34528> PMID: 27708393;
50. Toni N, Laplagne DA, Zhao C, Lombardi G, Ribak CE, Gage FH, et al. Neurons born in the adult dentate gyrus form functional synapses with target cells. *Nat Neurosci*. 2008; 11(8):901–7. Epub 2008/07/16. <https://doi.org/10.1038/nn.2156> PMID: 18622400;
51. Faulkner RL, Jang MH, Liu XB, Duan X, Sailor KA, Kim JY, et al. Development of hippocampal mossy fiber synaptic outputs by new neurons in the adult brain. *Proc Natl Acad Sci U S A*. 2008; 105(37):14157–62. Epub 2008/09/11. <https://doi.org/10.1073/pnas.0806658105> PMID: 18780780;
52. Toni N, Sultan S. Synapse formation on adult-born hippocampal neurons. *Eur J Neurosci*. 2011; 33(6):1062–8. Epub 2011/03/15. <https://doi.org/10.1111/j.1460-9568.2011.07604.x> PMID: 21395849.
53. Bergami M, Berninger B. A fight for survival: the challenges faced by a newborn neuron integrating in the adult hippocampus. *Dev Neurobiol*. 2012; 72(7):1016–31. <https://doi.org/10.1002/dneu.22025> PMID: 22488787.
54. Sivakumaran S, Mohajerani MH, Cherubini E. At immature mossy-fiber-CA3 synapses, correlated pre-synaptic and postsynaptic activity persistently enhances GABA release and network excitability via BDNF and cAMP-dependent PKA. *J Neurosci*. 2009; 29(8):2637–47. Epub 2009/02/27. <https://doi.org/10.1523/JNEUROSCI.5019-08.2009> PMID: 19244539.
55. Acsady L, Kamondi A, Sik A, Freund T, Buzsaki G. GABAergic cells are the major postsynaptic targets of mossy fibers in the rat hippocampus. *J Neurosci*. 1998; 18(9):3386–403. PMID: 9547246.
56. Brandt A, Striessnig J, Moser T. CaV1.3 channels are essential for development and presynaptic activity of cochlear inner hair cells. *J Neurosci*. 2003; 23(34):10832–40. PMID: 14645476.
57. Zhang Z, He Y, Tuteja D, Xu D, Timofeyev V, Zhang Q, et al. Functional roles of Cav1.3(alpha1D) calcium channels in atria: insights gained from gene-targeted null mutant mice. *Circulation*. 2005; 112(13):1936–44. <https://doi.org/10.1161/CIRCULATIONAHA.105.540070> PMID: 16172271.
58. Jacobo SM, Guerra ML, Hockerman GH. Cav1.2 and Cav1.3 are differentially coupled to glucagon-like peptide-1 potentiation of glucose-stimulated insulin secretion in the pancreatic beta-cell line INS-1. *J Pharmacol Exp Ther*. 2009; 331(2):724–32. <https://doi.org/10.1124/jpet.109.158519> PMID: 19710366;
59. Muller C, Mas Gomez N, Ruth P, Strauss O. CaV1.3 L-type channels, maxiK Ca(2+)-dependent K(+) channels and bestrophin-1 regulate rhythmic photoreceptor outer segment phagocytosis by retinal pigment epithelial cells. *Cell Signal*. 2014; 26(5):968–78. Epub 2014/01/11. <https://doi.org/10.1016/j.cellsig.2013.12.021> PMID: 24407175.
60. Clark NC, Nagano N, Kuenzi FM, Jarolimex W, Huber I, Walter D, et al. Neurological phenotype and synaptic function in mice lacking the CaV1.3 alpha subunit of neuronal L-type voltage-dependent Ca<sup>2+</sup> channels. *Neuroscience*. 2003; 120(2):435–42. PMID: 12890513.
61. Wong ST, Athos J, Figueroa XA, Pineda VV, Schaefer ML, Chavkin CC, et al. Calcium-stimulated adenylyl cyclase activity is critical for hippocampus-dependent long-term memory and late phase LTP. *Neuron*. 1999; 23(4):787–98. Epub 1999/09/11. PMID: 10482244.
62. Busquet P, Nguyen NK, Schmid E, Tanimoto N, Seeliger MW, Ben-Yosef T, et al. CaV1.3 L-type Ca<sup>2+</sup> channels modulate depression-like behaviour in mice independent of deaf phenotype. *Int J Neuropsychopharmacol*. 2010; 13(4):499–513. <https://doi.org/10.1017/S1461145709990368> PMID: 19664321.
63. Jessberger S, Clark RE, Broadbent NJ, Clemenson GD Jr., Consiglio A, Lie DC, et al. Dentate gyrus-specific knockdown of adult neurogenesis impairs spatial and object recognition memory in adult rats. *Learn Mem*. 2009; 16(2):147–54. <https://doi.org/10.1101/lm.1172609> PMID: 19181621;
64. Broadbent NJ, Gaskin S, Squire LR, Clark RE. Object recognition memory and the rodent hippocampus. *Learn Mem*. 2010; 17(1):5–11. <https://doi.org/10.1101/lm.1650110> PMID: 20028732;
65. Antunes M, Biala G. The novel object recognition memory: neurobiology, test procedure, and its modifications. *Cognitive Processing*. 2012; 13(2):93–110. <https://doi.org/10.1007/s10339-011-0430-z> PMID: 22160349
66. Lee I, Kesner RP. Differential contributions of dorsal hippocampal subregions to memory acquisition and retrieval in contextual fear-conditioning. *Hippocampus*. 2004; 14(3):301–10. <https://doi.org/10.1002/hipo.10177> PMID: 15132429

67. Fanselow MS, Dong HW. Are the dorsal and ventral hippocampus functionally distinct structures? *Neuron*. 2010; 65(1):7–19. <https://doi.org/10.1016/j.neuron.2009.11.031> PMID: 20152109;
68. Kitamura T, Saitoh Y, Takashima N, Murayama A, Niibori Y, Ageta H, et al. Adult neurogenesis modulates the hippocampus-dependent period of associative fear memory. *Cell*. 2009; 139(4):814–27. Epub 2009/11/17. <https://doi.org/10.1016/j.cell.2009.10.020> PMID: 19914173.
69. Tashiro A, Zhao C, Gage FH. Retrovirus-mediated single-cell gene knockout technique in adult newborn neurons in vivo. *Nat Protoc*. 2006; 1(6):3049–55. <https://doi.org/10.1038/nprot.2006.473> PMID: 17406567.
70. Vinet J, Sik A. Expression pattern of voltage-dependent calcium channel subunits in hippocampal inhibitory neurons in mice. *Neuroscience*. 2006; 143(1):189–212. Epub 2006/08/30. <https://doi.org/10.1016/j.neuroscience.2006.07.019> PMID: 16938402.
71. Darcy DP, Isaacson JS. L-type calcium channels govern calcium signaling in migrating newborn neurons in the postnatal olfactory bulb. *J Neurosci*. 2009; 29(8):2510–8. <https://doi.org/10.1523/JNEUROSCI.5333-08.2009> PMID: 19244525;
72. Goncalves JT, Schafer ST, Gage FH. Adult Neurogenesis in the Hippocampus: From Stem Cells to Behavior. *Cell*. 2016; 167(4):897–914. Epub 2016/11/05. <https://doi.org/10.1016/j.cell.2016.10.021> PMID: 27814520.
73. Krueger JN, Moore SJ, Parent R, McKinney BC, Lee A, Murphy GG. A novel mouse model of the aged brain: Over-expression of the L-type voltage-gated calcium channel Ca<sub>v</sub>(v)1.3. *Behavioural Brain Research*. 2017; 322:241–9. <https://doi.org/10.1016/j.bbr.2016.06.054> PMID: 27368417
74. Shitaka Y, Matsuki N, Saito H, Katsuki H. Basic fibroblast growth factor increases functional L-type Ca<sub>2+</sub> channels in fetal rat hippocampal neurons: implications for neurite morphogenesis in vitro. *J Neurosci*. 1996; 16(20):6476–89. PMID: 8815926.
75. Ikegaya Y. Abnormal targeting of developing hippocampal mossy fibers after epileptiform activities via L-type Ca<sub>2+</sub> channel activation in vitro. *J Neurosci*. 1999; 19(2):802–12. PMID: 9880600.
76. Schindelholz B, Reber BF. L-type Ca<sub>2+</sub> channels and purinergic P2X<sub>2</sub> cation channels participate in calcium-tyrosine kinase-mediated PC12 growth cone arrest. *Eur J Neurosci*. 2000; 12(1):194–204. Epub 2000/01/29. PMID: 10651874.
77. Boukhaddaoui H, Sieso V, Scamps F, Vignes S, Roig A, Valmier J. Q- and L-type calcium channels control the development of calbindin phenotype in hippocampal pyramidal neurons in vitro. *Eur J Neurosci*. 2000; 12(6):2068–78. PMID: 10886346.
78. Homma K, Kitamura Y, Ogawa H, Oka K. Serotonin induces the increase in intracellular Ca<sub>2+</sub> that enhances neurite outgrowth in PC12 cells via activation of 5-HT<sub>3</sub> receptors and voltage-gated calcium channels. *J Neurosci Res*. 2006; 84(2):316–25. Epub 2006/05/12. <https://doi.org/10.1002/jnr.20894> PMID: 16688720.
79. Zucca S, Valenzuela CF. Low concentrations of alcohol inhibit BDNF-dependent GABAergic plasticity via L-type Ca<sub>2+</sub> channel inhibition in developing CA3 hippocampal pyramidal neurons. *J Neurosci*. 2010; 30(19):6776–81. <https://doi.org/10.1523/JNEUROSCI.5405-09.2010> PMID: 20463239;
80. Lichvarova L, Jaskova K, Lacinova L. NGF-induced neurite outgrowth in PC12 cells is independent of calcium entry through L-type calcium channels. *Gen Physiol Biophys*. 2012; 31(4):473–8. Epub 2012/12/21. [https://doi.org/10.4149/gpb\\_2012\\_054](https://doi.org/10.4149/gpb_2012_054) PMID: 23255675.
81. Huang CY, Chu D, Hwang WC, Tsauro ML. Coexpression of high-voltage-activated ion channels Kv3.4 and Cav1.2 in pioneer axons during pathfinding in the developing rat forebrain. *J Comp Neurol*. 2012; 520(16):3650–72. <https://doi.org/10.1002/cne.23119> PMID: 22473424.
82. Hirtz JJ, Braun N, Griesemer D, Hannes C, Janz K, Lohrke S, et al. Synaptic refinement of an inhibitory topographic map in the auditory brainstem requires functional Cav1.3 calcium channels. *J Neurosci*. 2012; 32(42):14602–16. <https://doi.org/10.1523/JNEUROSCI.0765-12.2012> PMID: 23077046.
83. Duveau V, Laustela S, Barth L, Gianolini F, Vogt KE, Keist R, et al. Spatiotemporal specificity of GABAA receptor-mediated regulation of adult hippocampal neurogenesis. *Eur J Neurosci*. 2011; 34(3):362–73. <https://doi.org/10.1111/j.1460-9568.2011.07782.x> PMID: 21722213;
84. Winner B, Melrose HL, Zhao C, Hinkle KM, Yue M, Kent C, et al. Adult neurogenesis and neurite outgrowth are impaired in LRRK2 G2019S mice. *Neurobiol Dis*. 2011; 41(3):706–16. Epub 2010/12/21. <https://doi.org/10.1016/j.nbd.2010.12.008> PMID: 21168496;
85. Li T, Pan YW, Wang W, Abel G, Zou J, Xu L, et al. Targeted deletion of the ERK5 MAP kinase impairs neuronal differentiation, migration, and survival during adult neurogenesis in the olfactory bulb. *PLoS One*. 2013; 8(4):e61948. <https://doi.org/10.1371/journal.pone.0061948> PMID: 23630619;
86. Schnell E, Long TH, Bensen AL, Washburn EK, Westbrook GL. Neuroligin-1 knockdown reduces survival of adult-generated newborn hippocampal neurons. *Front Neurosci*. 2014; 8:71. <https://doi.org/10.3389/fnins.2014.00071> PMID: 24782702;



87. Carlson SW, Madathil SK, Sama DM, Gao X, Chen J, Saatman KE. Conditional overexpression of insulin-like growth factor-1 enhances hippocampal neurogenesis and restores immature neuron dendritic processes after traumatic brain injury. *J Neuropathol Exp Neurol*. 2014; 73(8):734–46. Epub 2014/07/09. <https://doi.org/10.1097/NEN.0000000000000092> PMID: 25003234;
88. Ren Z, Sahir N, Murakami S, Luellen BA, Earnheart JC, Lal R, et al. Defects in dendrite and spine maturation and synaptogenesis associated with an anxious-depressive-like phenotype of GABAA receptor-deficient mice. *Neuropharmacology*. 2015; 88:171–9. Epub 2014/08/12. <https://doi.org/10.1016/j.neuropharm.2014.07.019> PMID: 25107590;
89. Martel G, Uchida S, Hevi C, Chevere-Torres I, Fuentes I, Park YJ, et al. Genetic Demonstration of a Role for Stathmin in Adult Hippocampal Neurogenesis, Spinogenesis, and NMDA Receptor-Dependent Memory. *J Neurosci*. 2016; 36(4):1185–202. Epub 2016/01/29. <https://doi.org/10.1523/JNEUROSCI.4541-14.2016> PMID: 26818507;
90. Suzuki A, Josselyn SA, Frankland PW, Masushige S, Silva AJ, Kida S. Memory reconsolidation and extinction have distinct temporal and biochemical signatures. *J Neurosci*. 2004; 24(20):4787–95. Epub 2004/05/21. <https://doi.org/10.1523/JNEUROSCI.5491-03.2004> PMID: 15152039.
91. McHugh TJ, Tonegawa S. CA3 NMDA receptors are required for the rapid formation of a salient contextual representation. *Hippocampus*. 2009; 19(12):1153–8. <https://doi.org/10.1002/hipo.20684> PMID: 19650121;
92. Matus-Amat P, Higgins EA, Barrientos RM, Rudy JW. The role of the dorsal hippocampus in the acquisition and retrieval of context memory representations. *J Neurosci*. 2004; 24(10):2431–9. <https://doi.org/10.1523/JNEUROSCI.1598-03.2004> PMID: 15014118.
93. Melik E, Babar E, Ozen E, Ozgunen T. Hypofunction of the dorsal hippocampal NMDA receptors impairs retrieval of memory to partially presented foreground context in a single-trial fear conditioning in rats. *Eur Neuropsychopharmacol*. 2006; 16(4):241–7. <https://doi.org/10.1016/j.euroneuro.2005.07.008>
94. Matus-Amat P, Higgins EA, Sprunger D, Wright-Hardesty K, Rudy JW. The role of dorsal hippocampus and basolateral amygdala NMDA receptors in the acquisition and retrieval of context and contextual fear memories. *Behav Neurosci*. 2007; 121(4):721–31. <https://doi.org/10.1037/0735-7044.121.4.721> PMID: 17663597.
95. Schenberg EE, Oliveira MG. Effects of pre or posttraining dorsal hippocampus D-AP5 injection on fear conditioning to tone, background, and foreground context. *Hippocampus*. 2008; 18(11):1089–93. <https://doi.org/10.1002/hipo.20475>
96. Chang SD, Liang KC. The hippocampus integrates context and shock into a configural memory in contextual fear conditioning. *Hippocampus*. 2017; 27(2):145–55. Epub 2016/11/03. <https://doi.org/10.1002/hipo.22679> PMID: 27806432.
97. Hobin JA, Ji J, Maren S. Ventral hippocampal muscimol disrupts context-specific fear memory retrieval after extinction in rats. *Hippocampus*. 2006; 16(2):174–82. <https://doi.org/10.1002/hipo.20144> PMID: 16358312.
98. Xu C, Krabbe S, Grundemann J, Botta P, Fadok JP, Osakada F, et al. Distinct Hippocampal Pathways Mediate Dissociable Roles of Context in Memory Retrieval. *Cell*. 2016; 167(4):961–72.e16. Epub 2016/10/25. <https://doi.org/10.1016/j.cell.2016.09.051> PMID: 27773481.
99. Steullet P, Cabungcal JH, Kulak A, Kraftsik R, Chen Y, Dalton TP, et al. Redox dysregulation affects the ventral but not dorsal hippocampus: impairment of parvalbumin neurons, gamma oscillations, and related behaviors. *J Neurosci*. 2010; 30(7):2547–58. <https://doi.org/10.1523/JNEUROSCI.3857-09.2010> PMID: 20164340.
100. Cao L, Jiao X, Zuzga DS, Liu Y, Fong DM, Young D, et al. VEGF links hippocampal activity with neurogenesis, learning and memory. *Nat Genet*. 2004; 36(8):827–35. <https://doi.org/10.1038/ng1395> PMID: 15258583.
101. Li B, Wanka L, Blanchard J, Liu F, Chohan MO, Iqbal K, et al. Neurotrophic peptides incorporating adamantane improve learning and memory, promote neurogenesis and synaptic plasticity in mice. *FEBS Lett*. 2010; 584(15):3359–65. Epub 2010/07/06. <https://doi.org/10.1016/j.febslet.2010.06.025> PMID: 20600002.
102. Hagemann TL, Paylor R, Messing A. Deficits in adult neurogenesis, contextual fear conditioning, and spatial learning in a Gfap mutant mouse model of Alexander disease. *J Neurosci*. 2013; 33(47):18698–706. <https://doi.org/10.1523/JNEUROSCI.3693-13.2013> PMID: 24259590;
103. Maurice T, Bayle J, Privat A. Learning impairment following acute administration of the calcium channel antagonist nimodipine in mice. *Behav Pharmacol*. 1995; 6(2):167–75. Epub 1995/03/01. PMID: 11224324.
104. Quevedo J, Vianna M, Daroit D, Born AG, Kuyven CR, Roesler R, et al. L-type voltage-dependent calcium channel blocker nifedipine enhances memory retention when infused into the hippocampus. *Neurobiol Learn Mem*. 1998; 69(3):320–5. <https://doi.org/10.1006/nlme.1998.3822> PMID: 9707493.



105. Lashgari R, Motamedi F, Zahedi Asl S, Shahidi S, Komaki A. Behavioral and electrophysiological studies of chronic oral administration of L-type calcium channel blocker verapamil on learning and memory in rats. *Behav Brain Res*. 2006; 171(2):324–8. <https://doi.org/10.1016/j.bbr.2006.04.013> PMID: 16707172.
106. Quartermain D, deSoria VG, Kwan A. Calcium Channel Antagonists Enhance Retention of Passive Avoidance and Maze Learning in Mice. *Neurobiology of Learning and Memory*. 2001; 75(1):77–90. <http://dx.doi.org/10.1006/nlme.1999.3958>. PMID: 11124048
107. Deisseroth K, Malenka RC. GABA excitation in the adult brain: a mechanism for excitation- neurogenesis coupling. *Neuron*. 2005; 47(6):775–7. Epub 2005/09/15. <https://doi.org/10.1016/j.neuron.2005.08.029> PMID: 16157270.
108. Zaben MJ, Gray WP. Neuropeptides and hippocampal neurogenesis. *Neuropeptides*. 2013; 47(6):431–8. Epub 2013/11/13. <https://doi.org/10.1016/j.npep.2013.10.002> PMID: 24215800.
109. Kriegstein A, Alvarez-Buylla A. The Glial Nature of Embryonic and Adult Neural Stem Cells. *Annual review of neuroscience*. 2009; 32:149–84. <https://doi.org/10.1146/annurev.neuro.051508.135600> PMID: 19555289.
110. Grabel L. Developmental origin of neural stem cells: the glial cell that could. *Stem Cell Rev*. 2012; 8(2):577–85. Epub 2012/02/22. <https://doi.org/10.1007/s12015-012-9349-8> PMID: 22350457.
111. Reemst K, Noctor SC, Lucassen PJ, Hol EM. The Indispensable Roles of Microglia and Astrocytes during Brain Development. *Front Hum Neurosci*. 2016; 10:566. Epub 2016/11/24. <https://doi.org/10.3389/fnhum.2016.00566> PMID: 27877121;